CHAPTER IV

RESULTS AND DISCUSSION

4.1 The physical properties of catalysts

4.1.1 XRD pattern of catalysts

4.1.1.1 XRD pattern of zeolite beta

The zeolite beta catalysts with the gel mole composition of $1SiO_2$: 0.0083 Al_2O_3: 0.73 TEAOH : 19 H_2O (Si/Al = 60) reported by J. Aguado *et al.* [12] were successfully synthesized. The powdered XRD patterns of zeolite beta with the Si/Al mole ratio in gel of 60 are shown in Figure 4.1. The broad diffraction peak of (101) plane was observed in the 2θ range of 6.5-8.5° indicating the presence of two isomorphs, A and B, in zeolite beta. The most intense sharp peak at 22.4° was assigned to the diffraction of (302) plane, suggesting the high craystallinity of the zeolite [12].

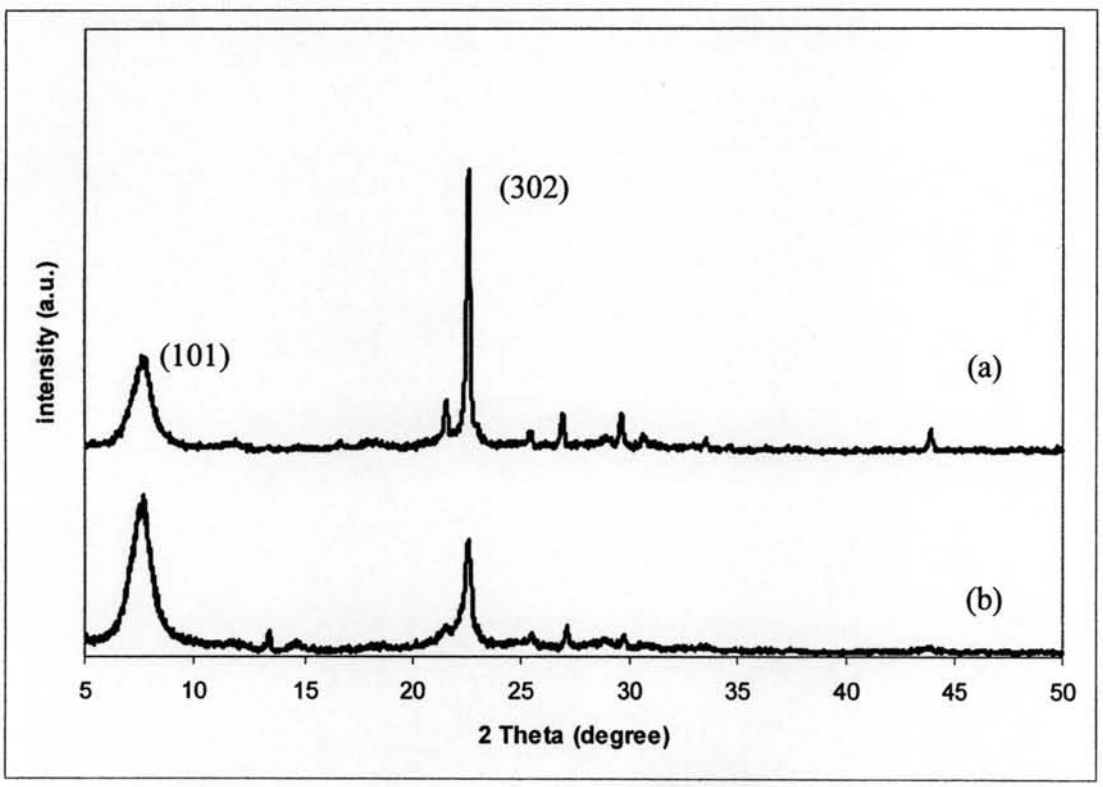

Figure 4.1 XRD patterns of (a) as-synthesizd and (b) calcined zeolite beta (Si/Al=60).

After the oxidative decomposition of template at 550°C for 10 h, the intensity of (302) peak at 22.4° was decreased due to dealumination of aluminium from the tetrahedral framework. It can be evidenced by the appearance of ^{27}Al-NMR signal of octahedral aluminum at 0 ppm, as shown in Figure 4.6.

4.1.1.2 XRD pattern of Al-HMS

Aluminum-containing hexagonal mesooporous silica (Al-HMS) with the Si/Al mole ratios in gel of 40 were synthesized with the gel mole composition of $1SiO_2$: 0.0125 Al_2O_3: 0.25 HDA: 8.3 EtOH: 100 H_2O reported by Tuel *et al* [43]. XRD patterns of as-synthsized and calcined Al-HMS (Si/Al= 40) are shown in Figure 4.2. A broad reflection peak of (100) at the 2θ range of 1.5–2.0° indicated the hexagonal mesoporous structure of HMS. After calcination in air at 550°C for 10 h, the hexagonal structure remained and the peak intensity increased, suggesting the removal of template from the pores of materials. Al-HMS with various Si/Al mole ratios in gel were also successfully synthesized. The XRD patterns of all calcined samples are demonstrated in Figure. 4.3. When aluminum was added to the HMS structure, the diffraction patterns of (100) peak shifted to the lower 2θ value suggesting the pore structure was wider due to the incorporation of aluminum in the silicate framework.

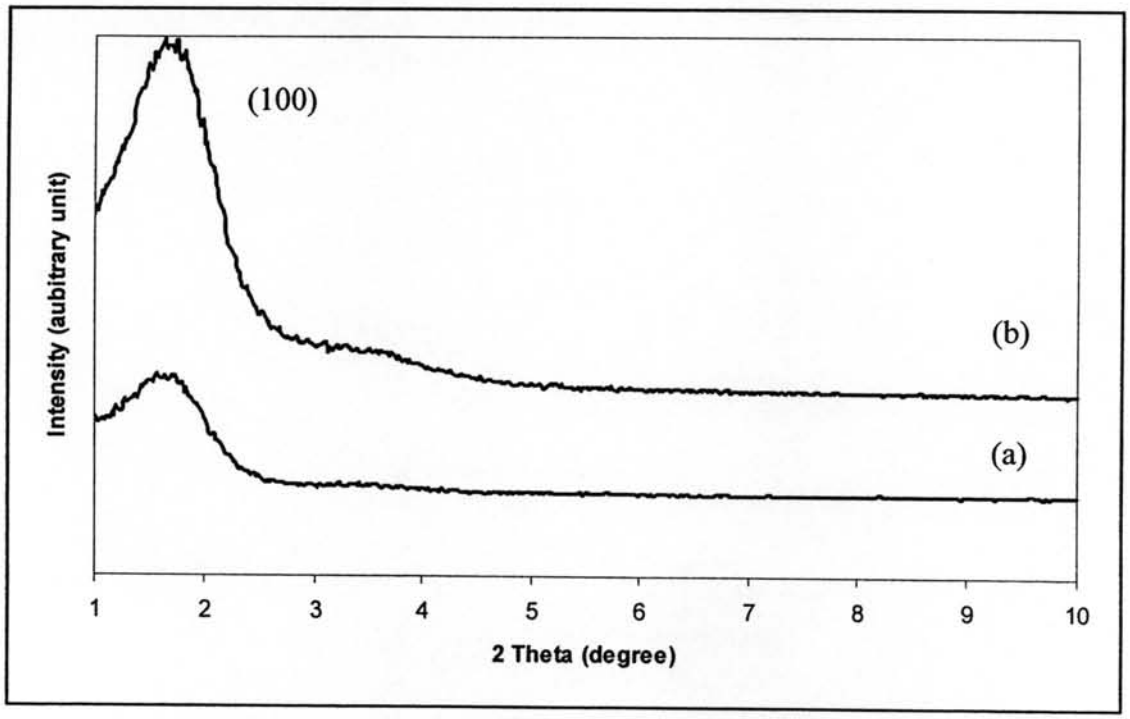

Figure 4.2 XRD patterns of (a) as-synthesizd and (b) calcined Al-HMS (Si/Al=40).

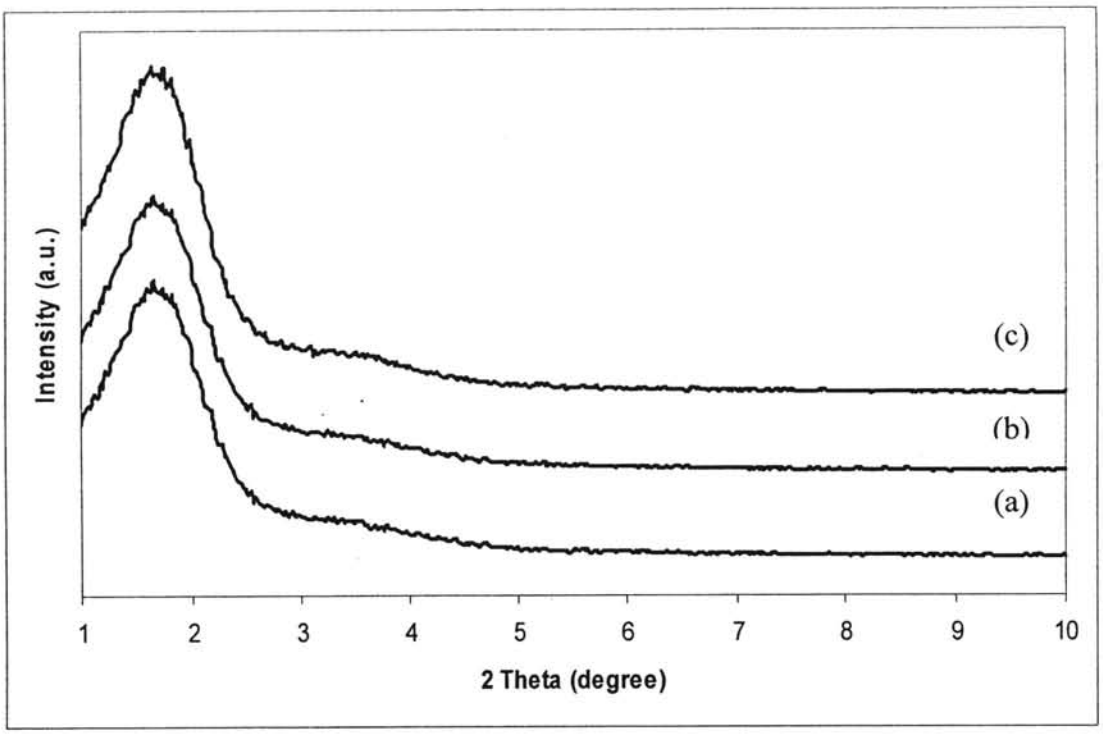

Figure 4.3 XRD patterns of (a) Al-HMS (Si/Al=40), (b) Al-HMS (Si/Al=60), and (c) Al-HMS (Si/Al=200).

4.1.2 SEM image of catalysts

4.1.2.1 SEM image of zeolite beta

The morphology of calcined zeolite beta prepared by ultrasonic irradiation technique is shown in Figure 4.4. Ordered round granular and shape of zeolite beta was observed with the average size of particles around 168 ± 5 nm.

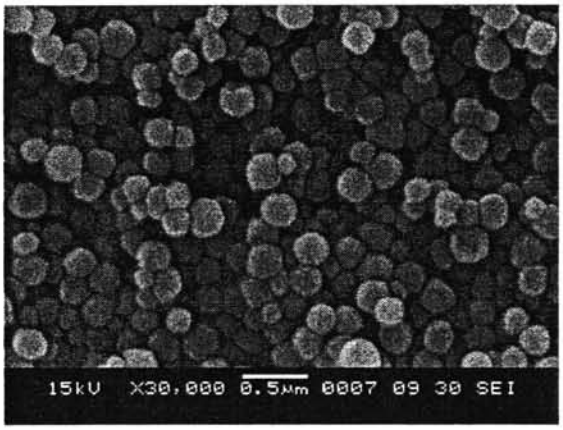

Figure 4.4 SEM image of zeolite beta (Si/Al=60).

4.1.2.2 SEM image of Al-HMS

Figure 4.5 shows the SEM images of Al-HMS with Si/Al mole ratios of 40, 60, and 200, respectively. All synthesized materials exhibited mixed morphology between crystalline particles and amorphous materials. However, the agglomerations of small amorphous particles were mainly observed. It was in agreement with the broad XRD peak of Al-HMS.

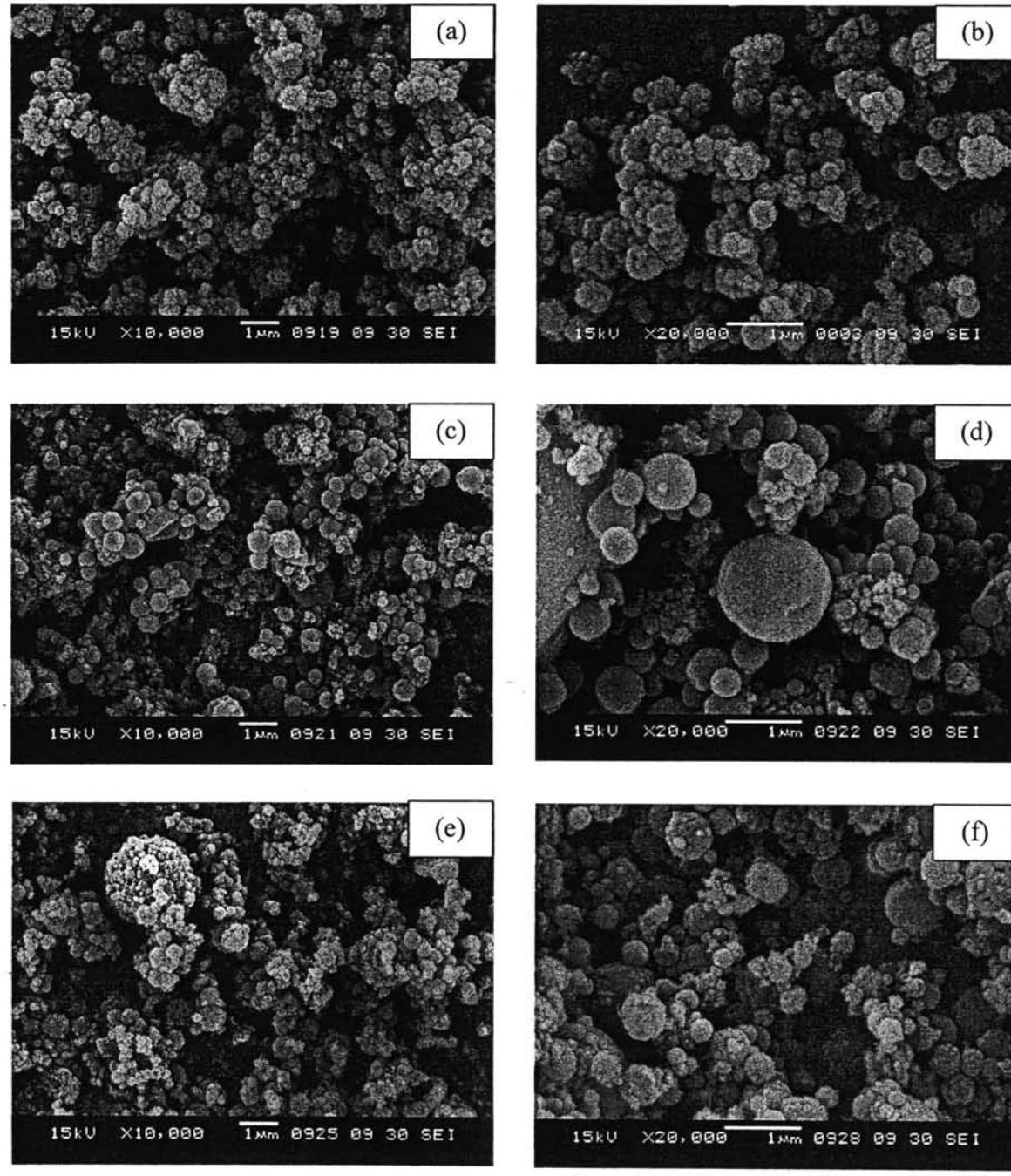

Figure 4.5 SEM images of Al-HMS with various Si/Al ratios in gel of (a)- (b) Si/Al=40, (c) - (d) Si/Al=60, and (e) -(f) Si/Al=200.

4.1.3 ^{27}Al-MAS-NMR Spectrum

4.1.3.1 ^{27}Al-MAS-NMR Spectrum of zeolite beta

The ^{27}Al-MAS-NMR spectrums of as-synthesized and calcined zeolite beta are displayed in Figure 4.6. The signal at 53 ppm is typically assigned to tetrahedrally coordinated (T_d) framework aluminum, and the peak at 0 ppm is assigned to the octahedrally coordinated (O_h) non-framework aluminum.

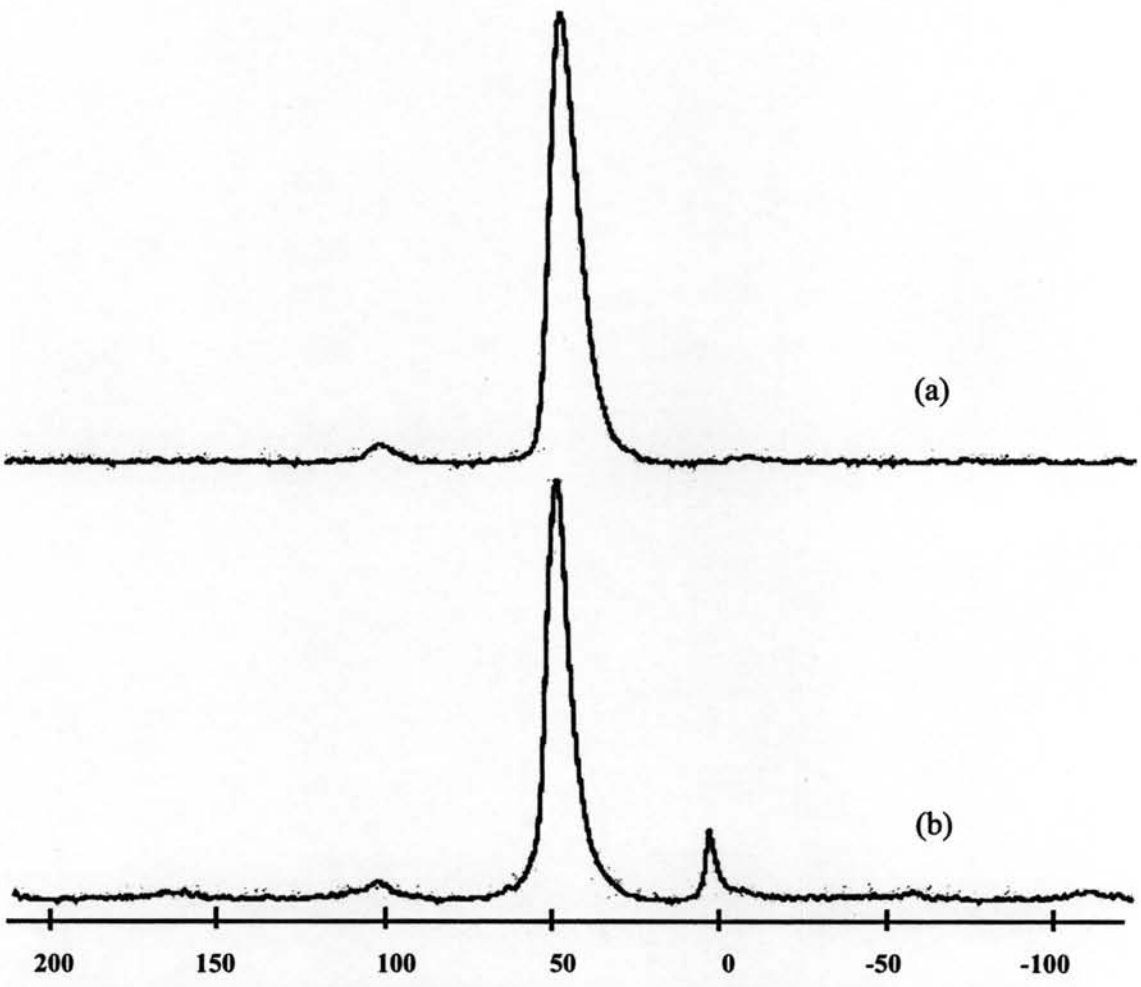

Figure 4.6 ^{27}Al-MAS-NMR spectrum of zeolite beta (a) as-synthesized, (b) calcined.

As-synthesized zeolite beta showed the ^{27}Al-MAS-NMR spectrum at 53 ppm. After calcination in air at 550°C for 6 h, the peak at 0 ppm appeared. The data demonstrated that before calcinations tetrahedral sites were occupied by aluminium atoms and after calcinations, dealumination of aluminium atoms from the framework occurred. Aluminium atoms in zeolite beta were located in the center of chains of framework, such a location resulted in highly strained environments of the aluminium sites and could account for their removal upon heating [53].

4.1.3.2 ^{27}Al-MAS-NMR Spectrum of Al-HMS

Figure 4.7 and 4.8 show the ^{27}Al-MAS-NMR spectrum of as-synthesized and calcined Al-HMS with various Si/Al ratios. The spectrum of as-synthesized samples showed a sharp resonance from four-coordinate aluminium at 53 ppm indicating that alumimium in synthetic gel mixture was incorporated into the framework. The weak signals at 0 ppm are due to octahedral aluminium. As aluminum content in the HMS structure increased, the signal intensity at the framework site increased. After calcined, Al-HMS samples still exhibited two signal peaks of octahedral and tetrahedral coordination. The depletion of peak intensity was caused by dealumination occurring during calcinations.

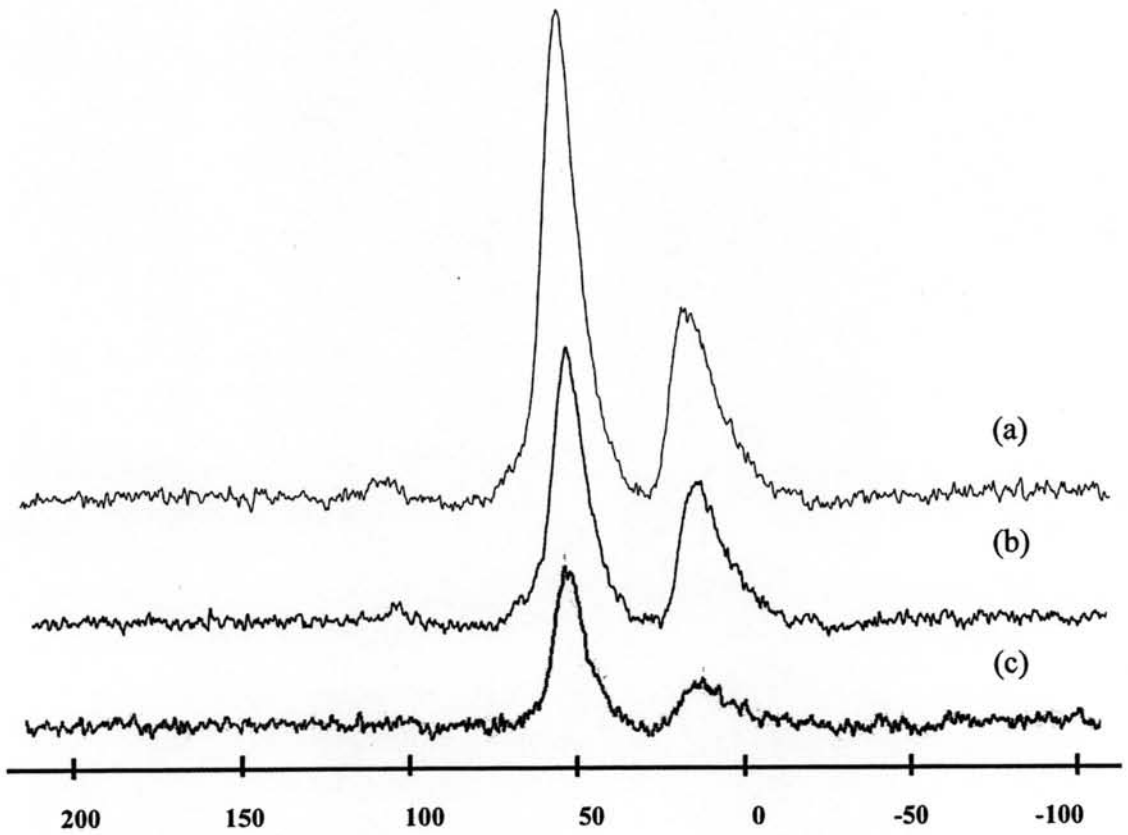

Figure 4.7 ^{27}Al-MAS-NMR spectrum of as-synthesized Al-HMS with different Si/Al ratios in gel (a) 40, (b) 60, and (c) 200.

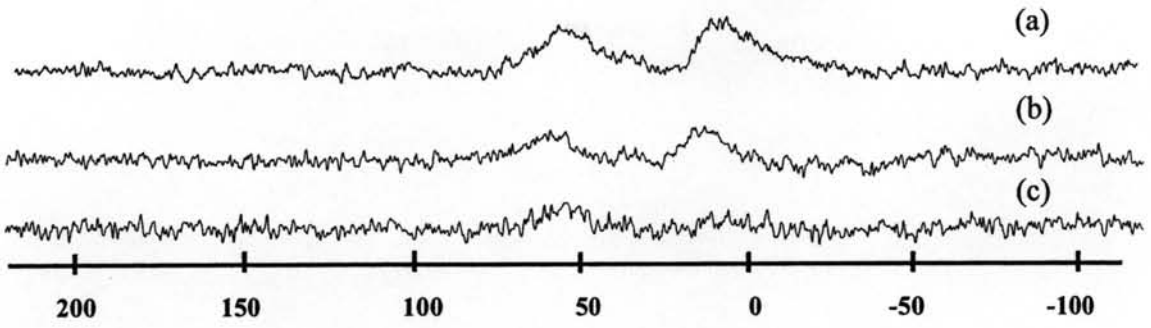

Figure 4.8 ^{27}Al-MAS-NMR spectrum of calcined Al-HMS with different Si/Al ratios in gel (A) 40, (B) 60, and (C) 200.

4.1.3.3 NH_4Cl treatment on Al-HMS

From Figure 4.8, it was concluded that all Al-HMS samples contained two signal peaks of octahedral and tetrahedral coordination. The octahedral aluminium can obscure the active site of catalysts and reduce the activity of catalyst. Therefore, to decrease the amount of octahedral aluminium, calcined Al-HMS samples were treated with NH_4Cl solution.

To obtain the optimal condition for NH_4Cl treatment, calcined Al-HMS (Si/Al= 40) was treated under different concentrations of NH_4Cl solution. The ^{27}Al-MAS-NMR spectrum of treated samples are displayed in Figure 4.9. Relative intensities of tetrahedral aluminium to octahedral aluminium were changed according to concentrations of NH_4Cl solution. When Al-HMS 40 was treated with 1, 2, and 3 M NH_4Cl concentrations (T1MAl-HMS 40, T2MAl-HMS 40, and T3MAl-HMS 40, respectively), the proportion of peak intensity at 53 ppm to peak intensity at 0 ppm increased, indicating aluminium atoms were incorporated into the framework. The relative ratios of Td/Oh calculated from peak area of ^{27}Al-MAS-NMR spectrum between tetrahedral aluminium and octahedral aluminium are summarized in Table 4.1.

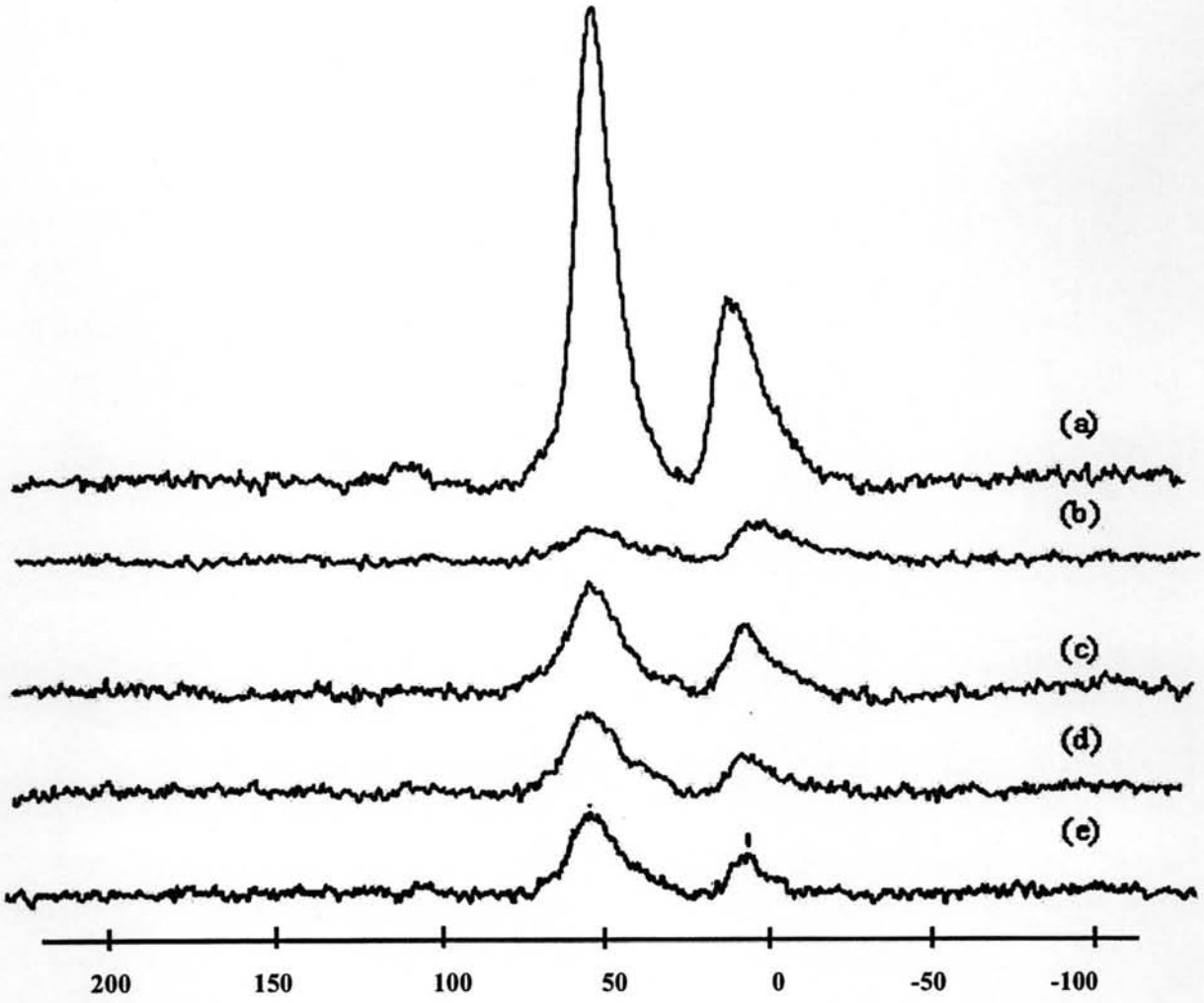

Figure 4.9 ^{27}Al-MAS-NMR spectrum of Al-HMS (Si/Al=40) before and after treatment with NH_4Cl for 3 h in various concentrations (a) as-synthesized (b) calcined-untreated, (c) 1 M, (d) 2 M, and (e) 3 M.

Table 4.1 Some properties of Al-HMS (Si/Al=40) before and after treated with NH_4Cl solution.

Sample of Al-HMS 40	S_{BET} (m^2/g)	Td/Oh[a]	Total acidity (mmol/g)
untreated Al-HMS 40	801	0.67	0.256
T1MAl-HMS 40	796	2.03	0.295
T2MAl-HMS 40	775	2.75	0.270
T3MAl-HMS 40	778	2.74	0.260

[a] Td/Oh was calculated from peak area between tetrahedral aluminium and octahedral aluminium in ^{27}Al-MAS-NMR spectrum.

From Table 4.1, the BET specific surface area of T1MAl-HMS 40 was similar to that of untreated one but Td/Oh and acidity were higher. It suggested that 1M NH_4Cl can reduced the non-framework aluminium without destroying the surface structure of Al-HMS. When the concentration of NH_4Cl increased, the BET specific surface area and acidity were relatively decreased whereas Td/Oh value increased. However, both surface area and Td/Oh values from T2MAl-HMS 40 and T3MAl-HMS 40 were not different. It may be due to the unstability of hexagonal structure when higher content of aluminium were incorporated. However, the activity in PP cracking over treated samples were performed at 350°C for 30 min in order to investigate the efficiency of treated sample. The results are shown in section 4.2.1.1

From the catalytic activity test, T1MAl-HMS 40 had higher activity than untreated sample and T2MAl-HMS 40. Therefore the optimal condition for ammonium treatment was the 1 M NH_4Cl solution for 1 g of catalyst to provide high relative intensity of tetrahedral aluminium to octahedral aluminium and high conversion for polyolefins cracking.

When Al-HMS with various Si/Al ratios were treated with 1M NH_4Cl, all of samples showed higher signal of tetrahedral aluminium at 53 ppm than the untreated samples, whereas the signal of octahedral were gradually decreased, as shown in Figure 4.9 and 4.10. As aluminum content increased, the signals at the framework site increased in intensity. For Al-HMS (Si/Al=200) the ^{27}Al-MAS-NMR spectrum of treated and untreated were not different because of low quantity of aluminium in catalyst, as shown in Figure 4.11.

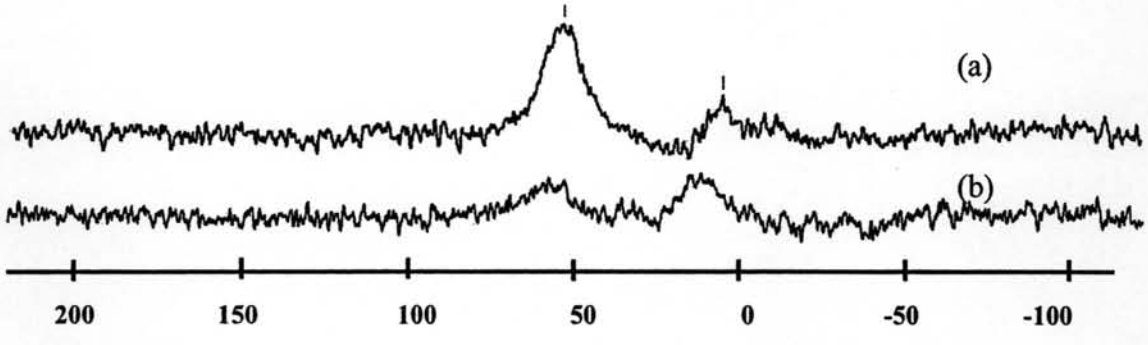

Figure 4.10 ^{27}Al-MAS-NMR spectrum of Al-HMS with Si/Al in gel of 60 were treated with 1 M NH_4Cl (a) treated (b) untreated.

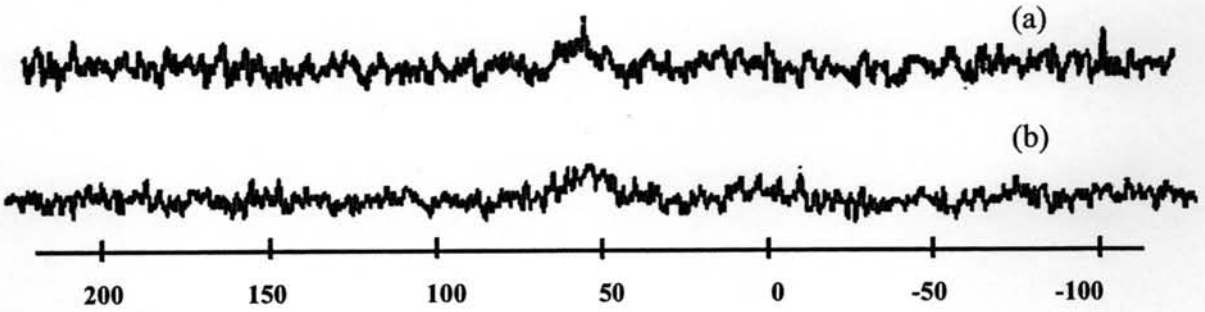

Figure 4.11 ^{27}Al-MAS-NMR spectrum of Al-HMS with Si/Al in gel of 200 were treated with 1 M NH_4Cl (a) treated (b) untreated.

4.1.4 Nitrogen Adsorption-Desorption of catalyst

4.1.4.1 Nitrogen Adsorption-Desorption of zeolite beta

The adsorption isotherm of zeolite beta in Figure 4.12 (a) indicated type I isotherm of microporous material. A rapid increase in adsorbed volume and a plateau were found at very low P/P_0. A small increase in the adsorbed volume was observed from P/P_0 = 0.9, suggesting the presence of a small amount of mesopores on the surface. Pore size distribution was calculated from the adsorption data by means of the MP plot method is displayed in Figure 4.12 (b). The narrow pore size distribution of the calcined zeolite beta sample was observed with the peak centered at 0.6 nm. Textural properties of calcined zeolite beta samples are summarized in Table 4.2.

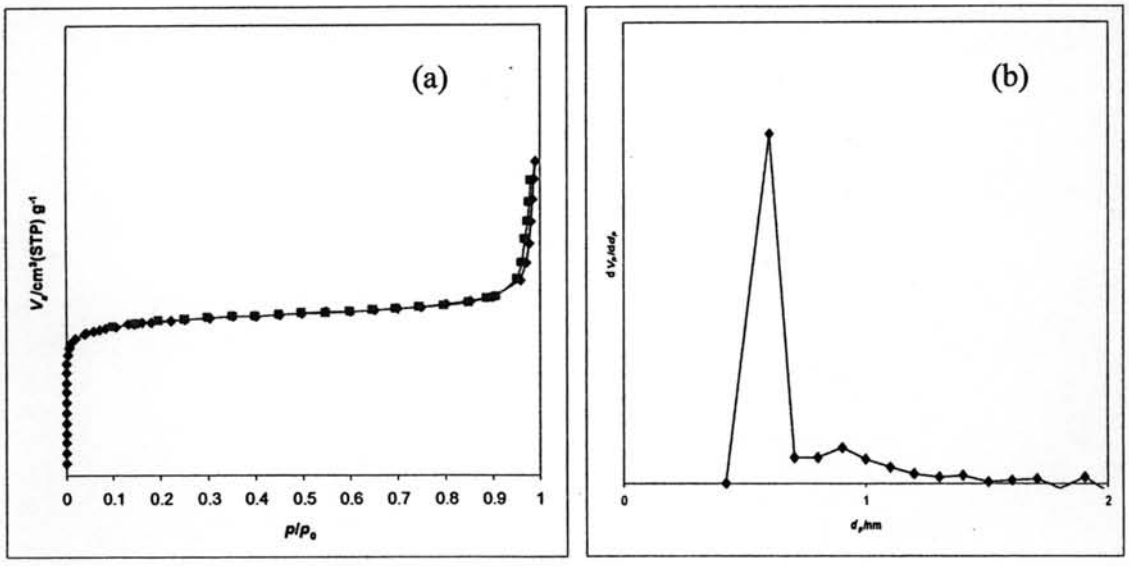

Figure 4.12 (a) N_2 adsorption-desorption isotherm (b) Pore-size distribution of zeolite beta (Si/Al=60).

4.1.4.2 Nitrogen Adsorption-Desorption of Al-HMS

The nitrogen-adsorption isotherms at 77 K for three calcined samples Al-HMS (Si/Al=40), Al-HMS (Si/Al=60), and Al-HMS (Si/Al=200) are illustrated in Figure 4.13. All Al-HMS samples presented a type IV isotherm in the IUPAC classification, and typical distributions for mesoporous material. The BET specific surface areas are listed in Table 4.2. The reduction of surface area was resulted from the wider pore structure of Al-HMS when aluminum species were incorporated into the HMS structure.

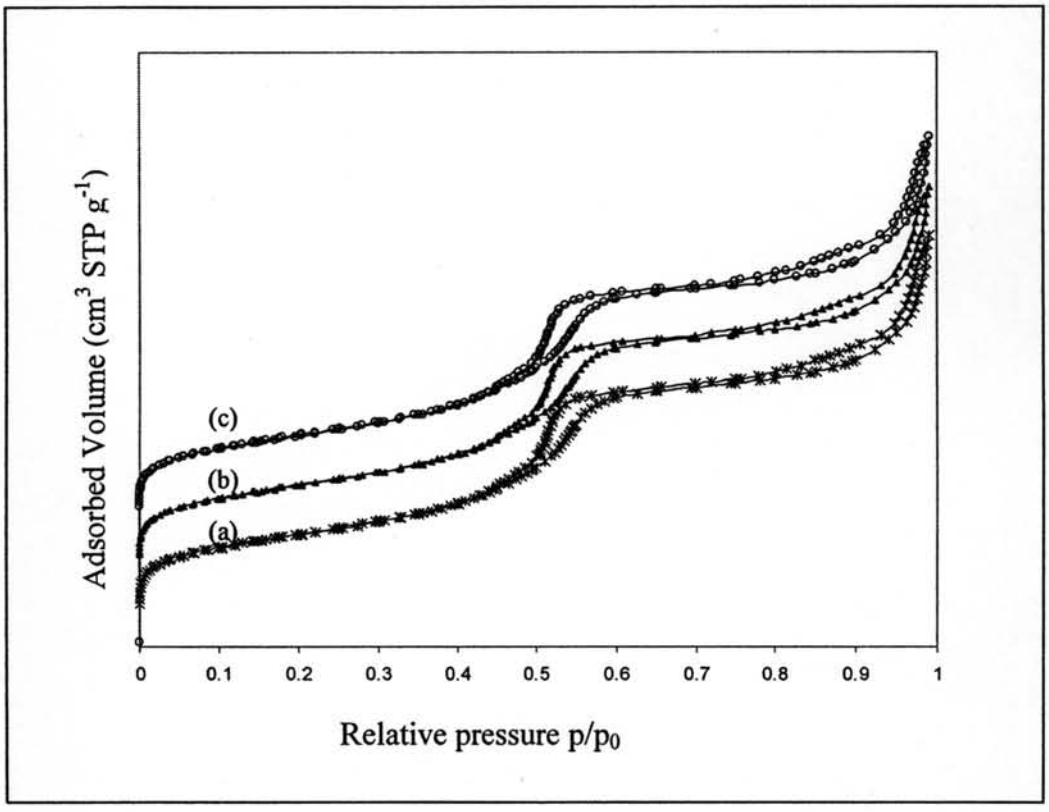

Figure 4.13 (a) N_2 adsorption-desorption isotherms of Al-HMS with various Si/Al ratios in catalyst of (a) 40, (b) 60, and (c) 200.

Pore size distribution was obtained from the adsorption data by means of the Barrett, Joyner and Halenda (BJH) method as shown in Figure 4.14. The pore size distributions of Al-HMS (Si/Al= 40 and 200) samples were narrow and centered at approximately 4.2 nm and those of Al-HMS (Si/Al = 60) was approximately 4.7 nm. Textural properties of Al-HMS samples are also displayed in Table 4.2.

Table 4.2 Textural properties of calcined zeolite beta and Al-HMS samples.

Sample	Si/Al mole ratio in gel	Before treatment		After treatment*	
		S_{BET} (m^2/g)	Pore volume (cm^3/g)	S_{BET} (m^2/g)	Pore volume (cm^3/g)
Zeolite beta	60	759	-	-	-
Al-HMS 40	40	801	1.7	796	1.7
Al-HMS 60	60	853	2.0	824	2.0
Al-HMS 200	200	876	1.7	872	1.7

*Treating with 1M NH_4Cl at boiling temperature for 3h.

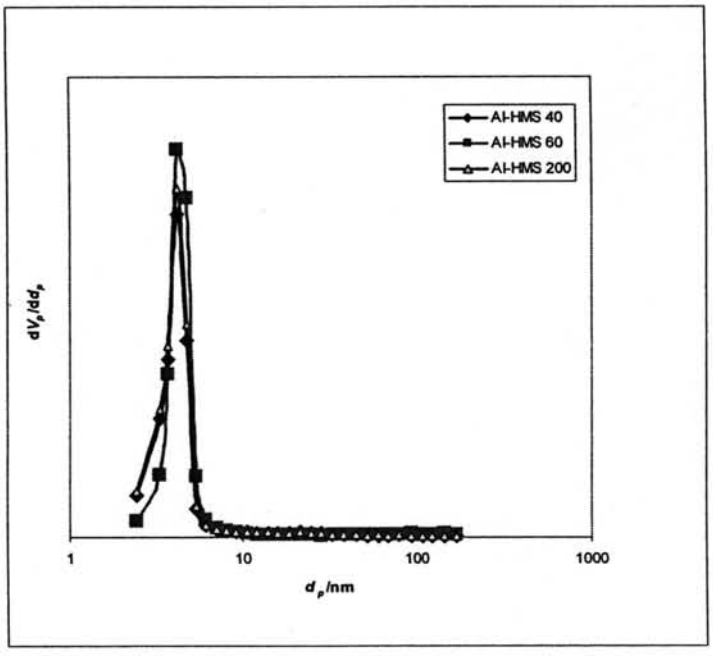

Figure 4.14 BJH pore-size distribution of Sample Al-HMS with various Si/Al ratios in catalyst.

4.1.5 Si/Al Ratios of catalysts

The Si/Al ratios in gel and in catalyst of zeolite beta and Al-HMS were compared in Table 4.3. The Si/Al mole ratios in catalyst for zeolite beta and Al-HMS catalysts synthesized by hydrothermal and sol-gel methods were less than found in gel by half. It indicated that aluminium atoms were incorporated in the catalyst. It was agreement with

^{27}Al-MAS-NMR spectrum that all aluminium were in tetrahedral and octahedral forms. The high acidity were obtained when increased aluminium content.

Table 4.3 Physicochemical properties of the catalysts.

Sample	Si/Al mole ratio in gel[a]	Si/Al mole ratio in catalyst[b]	Total acidity[c] (mmol/g)
Zeolite beta	60	27	0.721
Al-HMS 40	40	32	0.295
Al-HMS 60	60	39	0.249
Al-HMS 200	200	105	0.213

a: calculated from reagent quantities.

b: Aluminum (Al) was determined by ICP-AES and Si was calculated from the deduction of AlO_2 from the sample weight.

c: From ammonia TPD.

4.1.6 NH_3-TPD Profiles

Figure 4.15 shows the NH_3-TPD profiles of zeolite beta and treated Al-HMS. All samples exhibited two NH_3 desorption peaks corresponding to different acidity of the samples. The peak position corresponds to acid strength, while the peak area corresponds to number of acid site. The peak centered at 150°C was typically assigned to a weaker acid site, and the other one at 350°C was assigned to a stronger acid site. For Al-HMS, the number of weaker acid sites decreased when the Si/Al ratio increased due to the decrease in aluminum content in catalyst. The number of stronger acid site was pronounced as follows: T1M Al-HMS 40> T1M Al-HMS 60> T1M Al-HMS 200, respectively. The acidity of all Al-HMS samples were lower than the one observed in the zeolite beta. The quantities of adsorbed-desorbed ammonia were calculated and summarized in Table 4.3. These results confirmed that acid sites in Al-HMS were less than zeolite beta.

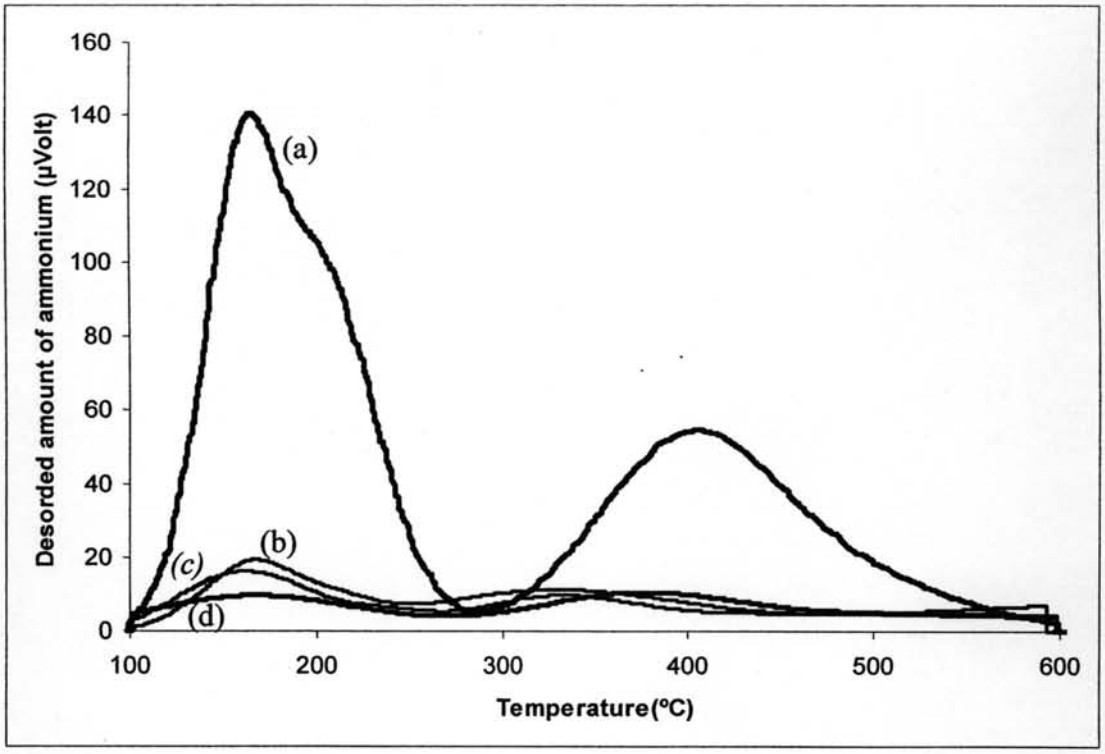

Figure 4.15 NH_3-TPD profiles of (a) zeolite beta and treated with 1 M NH_4Cl Al-HMS with different Si/Al ratios (b) 40, (c) 60, and (d) 200.

4.2 Activity of catalysts in PP cracking

4.2.1 Activity of Al-HMS catalysts in PP cracking

4.2.1.1 Effect of NH_4Cl treatment on Al-HMS

Cracking of PP over Al-HMS treated with 1M NH_4Cl (T1M Al-HMS 40) was conducted at 350°C comparing with untreated catalyst. The data are summarized in Table 4.4. T1MAl-HMS 40 catalyst gave a higher activity in PP conversion than untreated sample. The selectivity to gas fraction was not different while liquid fraction was slightly increased. It was owing to T1MAl-HMS 40 had a higher amount of aluminium in tetradedral framework than the untreated Al-HMS (Td/Oh of T1MAl-HMS 40 = 2.03 and Td/Oh of untreated sample = 0.67).

When the Al-HMS treated with 2M NH_4Cl (T2MAl-HMS) was compared, T1MAl-HMS 40 also had a higher activity than the T2MAl-HMS 40 sample. The selectivity to gas fraction was not different while liquid fraction was relatively decreased. Although T2MAl-HMS 40 had higher Td/Oh than T1MAl-HMS 40, surface area was lower. It was concluded that surface area also played an important role in catalytic activity. The polymers were left

in residue of all samples so yield of coke was not calculated. Thus, the optimal condition NH_4Cl treatment on Al-HMS was the reflux with 1M NH_4Cl at boiling temperature for 3 h. That condition was chosen for treating Al-HMS with various ratio of Si/Al.

Table 4.4 %Conversion and %yield obtained by catalytic cracking of PP over untreated and treated Al-HMS 40.

	Untreated Al-HMS 40	T1MAl-HMS 40	T2MAl-HMS 40
%Conversion*	72.2	78.8	73.4
%yield* 1. gas fraction	21.8	23	21.4
2. liquid fraction	50.4	55.8	52
3. residue	27.8	21.2	26.6
Total volume of liquid fraction (cm^3)	3.1	3.5	3.3
Liquid fraction density (g/cm^3)	0.74	0.73	0.73

Condition: 10 wt% of catalyst to plastic, N_2 flow of 20 cm^3/min, reaction temperature of 350°C, and reaction time of 30 min.*Deviation within 0.5% for conversion, 0.2% for yield of gas fraction, 0.6% for yield of liquid fraction, and 0.5% for yield of residue.

4.2.1.2 Effect of Si/Al ratios

Cracking of PP over treated Al-HMS catalysts with various Si/Al ratio were conducted at 350°C and the results are shown in Table 4.5. By increasing the aluminum content, %conversion increased. The selectivity to gas products, liquid products, and distillate oil also rise. These results explained that the increase in aluminium content accelerated the degradation of polymer proceeding through carbocation mechanism. A highest conversion of PP cracking at 78.7% was observed over T1MAl-HMS 40 (Si/Al = 40) and lower conversion over T1MAl-HMS 60 (Si/Al = 60) and T1MAl-HMS 200 (Si/Al = 200) at 70.6 % and 59.1%, respectively. Therefore, T1MAl-HMS 40 was chosen for further study as the zeolite beta/Al-HMS mixed catalyst.

Table 4.5 %Conversion, %yield, and %selectivity of liquid fraction obtained by catalytic cracking of PP over treated Al-HMS catalysts with various Si/Al ratios.

	T1MAl-HMS 40	T1MAl-HMS 60	T1MAl-HMS 200
%Conversion*	78.7	70.6	59.1
%yield* 1. gas fraction	23.1	19.7	17.6
2. liquid fraction	55.6	50.9	41.7
3. residue	21	29.4	40.9
%selectivity of liquid fraction			
1. distillate oil	*22.4*	*20.1*	*18.2*
2. heavy oil	*77.6*	*79.9*	*81.8*
Total volume of liquid fraction (cm^3)	3.52	3.3	2.8
Liquid fraction density (g/cm^3)	0.73	0.74	0.74

Condition: 10 wt% of catalyst to plastic, N_2 flow of 20 cm^3/min, reaction temperature of 350°C, and reaction time of 30 min. .*Deviation within 0.5% for conversion, 0.6% for yield of gas fraction, 0.6% for yield of liquid fraction, and 0.5% for yield of residue.

4.2.2 Activity of zeolite beta and Al-HMS mixed catalysts in PP cracking

4.2.2.1 Effect of Al-HMS ratio in mixed catalyst

Since T1MAl-HMS 40 gave the highest activity in PP cracking, it was chosen for studying the activity of mixed catalysts between zeolite beta and Al-HMS. The mixed catalyst were prepared by physical mixing with various ratio of T1M Al-HMS 40 as follows; 0%Al-HMS, 20%Al-HMS, 40%Al-HMS, 60%Al-HMS, 80%Al-HMS, 90%Al-HMS, 95%Al-HMS, and 100%Al-HMS. At 0%Al-HMS, it means pure zeolite beta does not mix with T1M Al-HMS 40 and same as 100%Al-HMS which means pure T1MAl-HMS 40 does not mix with zeolite beta.

Table 4.6 shows the catalytic conversion obtained at 350°C in the cracking of PP over different ratios of T1M Al-HMS 40 (Al-HMS) comparing with thermal cracking. At 0% Al-HMS (pure zeolite beta), the conversion was less than that of 100%Al-HMS. However, the selectivity to gas fraction and distillate oil were higher. In addition, conversions and yields of liquid fraction over mixed catalysts increased when the ratio of Al-HMS increased. Catalysts in the range of 90-100%Al-HMS gave almost 80% conversion whereas the activities obtained from 60-80%Al-HMS were approximately

60%conversion, and activities over 0-40%Al-HMS were around 50%conversion, which corresponds to the reducing of the residue yields. These results could be explained by structure and properties of mesoporous materials. Al-HMS had a wide pore size of 4.19 nm and surface area whereas zeolite beta had a pore size of 0.6 nm and lower surface area than Al-HMS. The large pore size of Al-HMS allowed large polymer molecules to access the pore better than zeolilte beta. The selectivity to gas products and distillate oil depended on proportion of Al-HMS. With increasing mesoporous content, yield of gas fraction and distillate oil reduced. It was due to the acidity of zeolite beta was reduced because of high proportion of Al-HMS.

Table 4.6 %Conversion, %yield, and %selectivity of liquid fraction obtained by thermal and catalytic cracking of PP over Sample zeolite beta/Al-HMS mixed catalysts with various Al-HMS ratios.

Sample	Thermal	0% Al-HMS	20% Al-HMS	40% Al-HMS	60% Al-HMS	80% Al-HMS	90% Al-HMS	95% Al-HMS	100% Al-HMS
%Conversion*	2.4	44.1	53.7	49.6	64.9	62.9	72.1	80.3	78.7
%yield*1. gas fraction	2.4	30.2	37.5	31.3	33.7	22.9	26.9	24.6	24.1
2. liquid fraction	-	13.9	16.1	18.3	31.2	40.0	45.3	55.7	54.6
3. residue	97.6	55.9	46.3	50.4	35.1	37.1	27.9	19.7	21.3
%selectivity of liquid fraction									
1. distillate oil	-	*71.6*	*64.8*	*59.9*	*52.3*	*49.0*	*40.4*	*37.2*	*22.4*
2. heavy oil	-	*28.8*	*35.2*	*40.1*	*47.7*	*51.0*	*59.6*	*62.9*	*77.6*
Total volume of liquid fraction (ml)	-	0.9	1.1	1.3	2.1	2.7	3.1	3.7	3.5
Liquid fraction density (g/ml)	-	0.68	0.71	0.71	0.73	0.73	0.73	0.73	0.73

Condition: 10 wt% of catalyst to plastic, N_2 flow of 20 cm^3/min, reaction temperature of 350°C, and reaction time of 30 min. *Deviation within 0.9% for conversion, 0.8% for yield of gas fraction, 1.1% for yield of liquid fraction, and 0.9% for yield of residue.

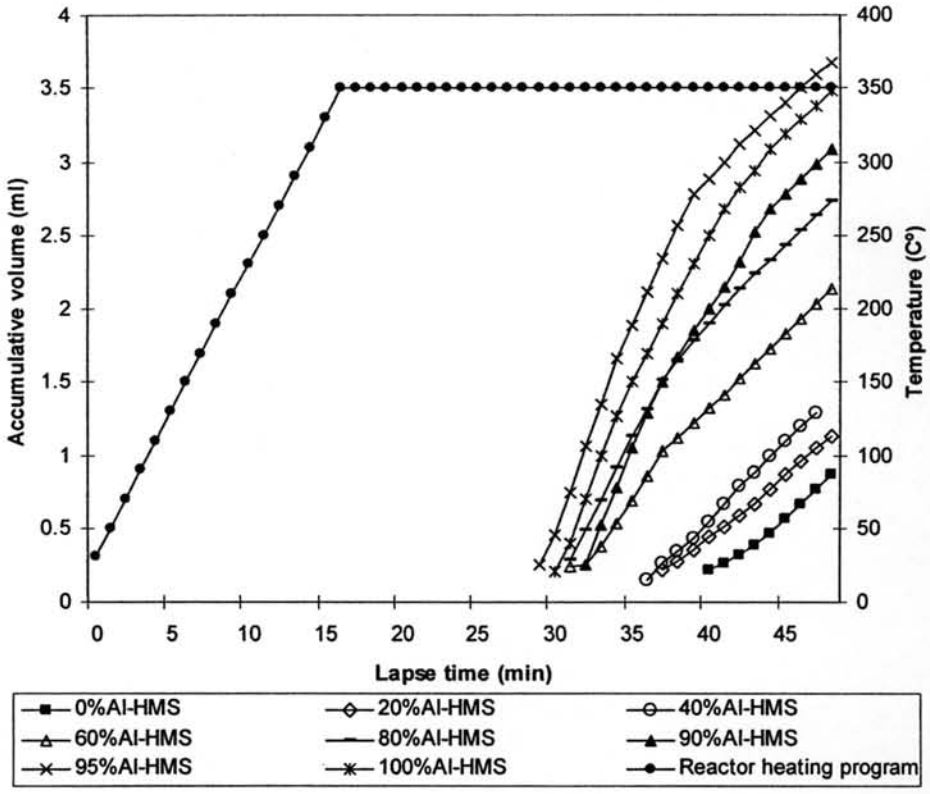

Figure 4.16 Accumulative volume of liquid fractions from catalytic cracking of PP over zeolite beta/Al-HMS mixed catalysts with various Al-HMS ratios.

In this work, it was observed that 95%Al-HMS showed the highest activity. These results could be explained by the mixing of microporous and mesoporous materials accelerated the cracking of PP better than the pure catalyst. The large pore size of Al-HMS allowed large polymer molecules to access the pore and broke the long polymeric chain from ends into small unit or oligomer. Then these oligomer diffused into pore and channel of zeolite and broke into smaller molecules [54]. It was also confirmed by the accumulative volumes of liquids obtained over mixed catalysts, which are displayed in Figure 4.16. In addition, the rates of high proportion of mesoporous material were much faster than those of low proportions.

The yields of gaseous products for PP cracking are shown in Figure 4.17. Considering only gases at ambient condition which were normally C_1 through C_5, the major component for thermal cracking were C_3 (propene), C_5 (n-pentane), C_2 (Ethane), C_4 (iso-butene) and C_5^+. For catalytic cracking major components were C_3 (propene), C_4 (iso-butane), C_4 (iso-butene), C_5 (iso-pentane) and C_5^+. However, the C_5^+ components from liquid vapors of C_6 (hexane) which had higher boiling point than that of C_5 (n-pentane) was obviously detected in a significant amount. The difference in gas components between

thermal and catalytic cracking was explained by the different cracking mechanism. Thermal cracking proceeded through random scission whereas catalytic cracking proceeded through carbocation [9].

The liquid products for catalytic cracking were found in broad range of C_6-C_9 as shown in Figure 4.18. It was observed that the main products of catalytic cracking were C_7.

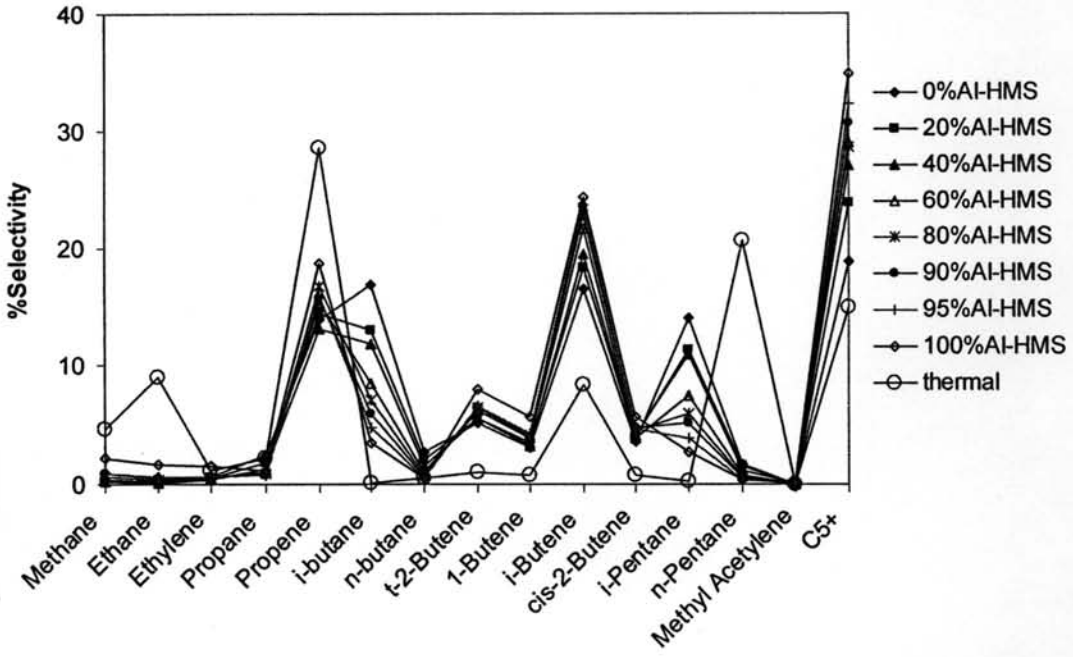

Figure 4.17 Distribution of gas fraction obtained by thermal and catalytic cracking of PP over zeolite beta/Al-HMS mixed catalysts with various Al-HMS ratios.

The product distribution of SUPELCO standard gasoline fraction are shown in Figure 4.19. The major components were C_7 and C_8. That was comparable to the distribution of distillate oil obtained in this work based on the boiling point range using n-paraffins as reference.

From this experiment, it was concluded that the activity in PP cracking over mixed catalyst depended on proportion of mesoporous material. The effect of the large pore size enhanced the activity and liquid fraction. However, the selectivity to products varied. If the process required gas and distillate oil products, the higher proportions of zeolite beta were appropriate. Also the process required liquid and heavy oil products, the higher proportions Al-HMS were suitable. In this research 95%Al-HMS gave highest conversion and high selectivity to liquid product. Therefore, 95%Al-HMS was chosen to study in this research.

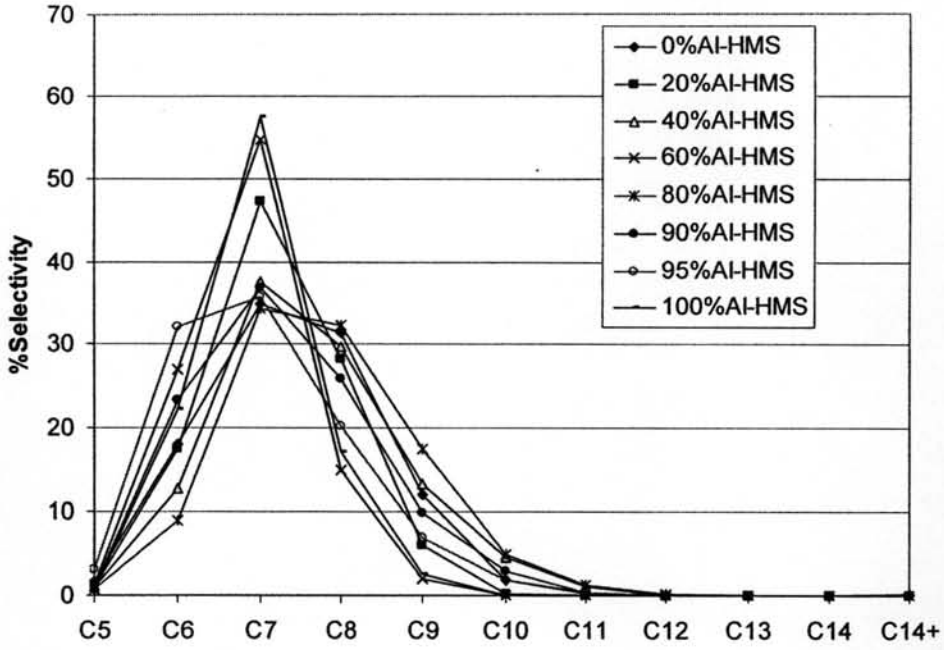

Figure 4.18 Carbon number distribution of distillate oil obtained catalytic cracking of PP over zeolite beta/Al-HMS mixed catalysts with various Al-HMS ratios.

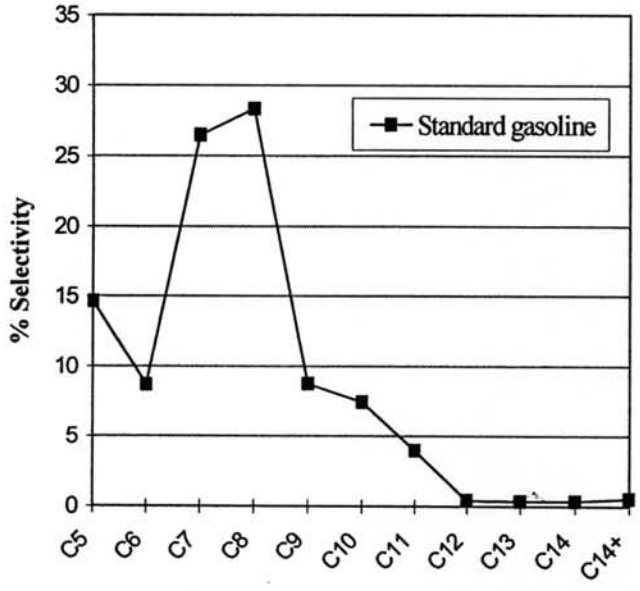

Figure 4.19 Carbon number distribution of commercial SUPELCO standard gasoline fraction.

4.2.1.2 Effect of plastic to catalyst ratios

To study the effect of plastic to catalyst ratios it's the activity, mixed zeolite beta/Al-HMS catalysts with 95%Al-HMS was chosen. The variations in plastic to catalyst ratio were studied in the range of 2.5-10%wt. The results are shown in Table 4.7. The

plastic conversion increased with increasing the catalysts loading in the reaction mixture. The selectivity to gas fraction did not much different, while liquid fraction increased. At low portion of catalyst, e.g. 2.5% weight of catalyst, the acidity of catalyst was minimized. The hindered molecules or the bulky polypropylene molecules were obstructed and could not diffuse into the pores. Besides, low acidity retarded the reaction on the external surface area of catalyst. It gave a high residue yield.

Table 4.7 %Conversion, %yield, and %selectivity of liquid fraction obtained by catalytic cracking of PP over the 95%Al-HMS mixed catalyst with various plastic to catalyst ratios.

	2.5%cat	5%cat	10%cat
%Conversion*	48.4	68.3	80.3
%yield* 1. gas fraction	21.5	27.5	25.7
2. liquid fraction	26.9	40.7	54.7
3. residue	51.6	31.7	19.7
%selectivity of liquid fraction			
1. distillate oil	*38.3*	*24.5*	*37.2*
2. heavy oil	*61.7*	*75.5*	*62.9*
Total volume of liquid fraction (ml)	1.8	2.8	3.7
Liquid fraction density (g/ml)	0.76	0.73	0.73

Condition: N_2 flow of 20 cm^3/min, reaction temperature of 350°C, and reaction time of 30 min. *Deviation within 0.9% for conversion, 0.5% for yield of gas fraction, 0.9% for yield of liquid fraction, and 0.9% for yield of residue.

Figure 4.20 shows the accumulative volume of liquid products and reaction temperature as function of lapse time. It was seen that the rate of accumulative liquid volumes obtained over 10% weight of catalyst was much faster than those of 5 and 2.5% weight of catalyst, respectively. These results suggested that the suitable of plastic to catalyst ratio accelerate the cracking of polymer.

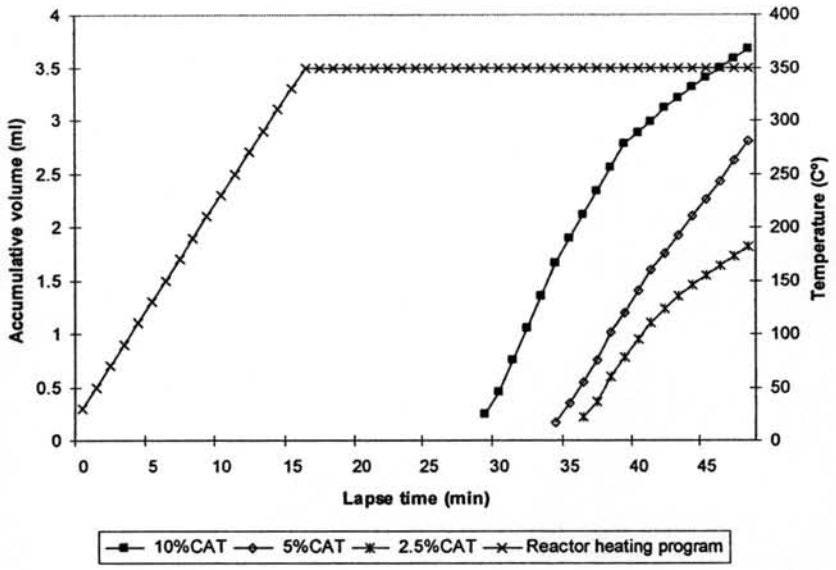

Figure 4.20 Accumulative volumes of liquid fractions from catalytic cracking of PP over the 95%Al-HMS mixed catalyst with various plastic to catalyst ratios.

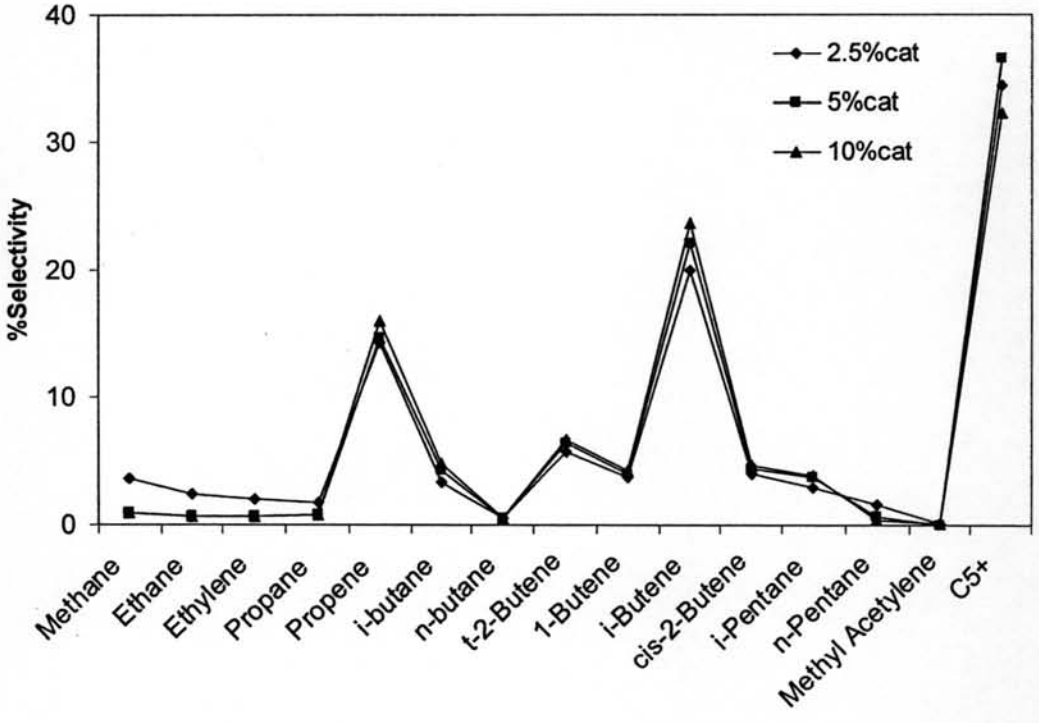

Figure 4.21 Distribution of gas fraction obtained by catalytic cracking of PP over the 95%Al-HMS mixed catalyst with various plastic to catalyst ratios.

The yields of gaseous products for PP cracking over 95%Al-HMS with various plastic to catalyst ratio were not different. The products were mainly C_3 (propene), C_4 (iso-butane), C_4 (iso-butene), C_5 (iso-pentane) and C_5^+ as shown in Figure 4.21.

Figure 4.22 shows the liquid products for catalytic cracking in broad range of C_6-C_9. The major product was C_7. However, liquid products from 95%Al-HMS with various plastic to catalyst ratios were in commercial gasoline range.

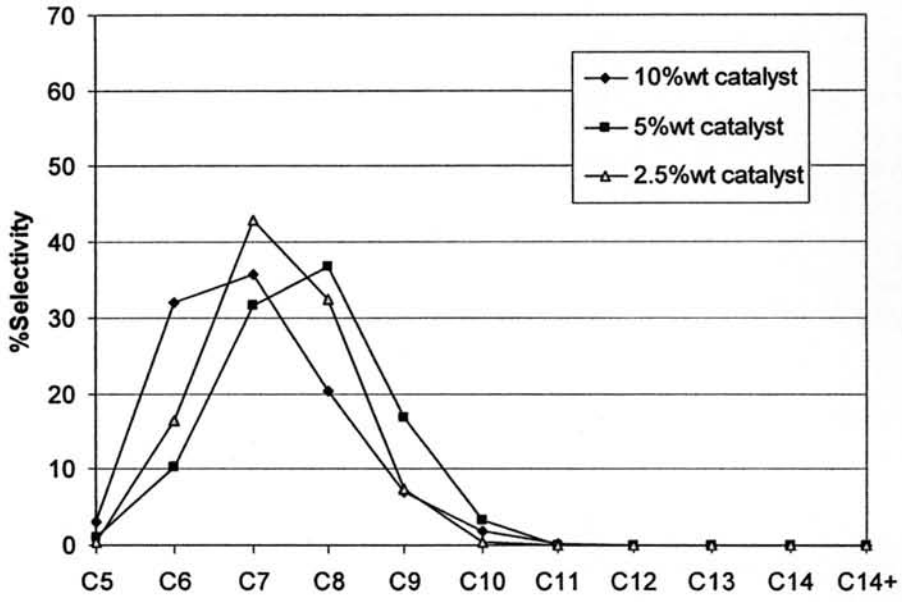

Figure 4.22 Carbon number distribution of distillate oil obtained by catalytic cracking of PP over the 95%Al-HMS mixed catalyst with various plastic to catalyst ratios.

According to the results of plastic to catalyst ratio in PP cracking, the 10% wt of catalyst was selected to be the test condition for further studies in this work due to a considerably high conversion and large amount of liquid fractions obtained.

4.2.1.3 Effect of temperature

The influence of reaction temperature in the range of 350-410°C was investigated using the 95%Al-HMS mixed catalyst, a catalyst to plastic ratio of 10. The data are displayed in Table 4.8. For thermal cracking, conversion was increased when temperature increased. It was obviously seen that the selectivity to gas and liquid products were increased. The high temperature enhanced the degradation of polymer. For catalytic cracking, conversion also increased in the similar way as thermal cracking. Comparing between thermal cracking and catalytic cracking at the same temperature, it was obvious

that catalytic cracking showed higher conversion than thermal cracking because the acidity of catalyst increased the degradation of polymer. At 350°C and 380°C, large difference in conversions between catalytic and thermal reaction were 77.9 and 80.7%, respectively. Whereas, at 410°C the difference in conversion was only 18%. It was suggested that at 380°C, the mixed catalyst exhibited the highest efficiency in PP cracking.

Table 4.8 %Conversion, %yield, and %selectivity of liquid fraction obtained by thermal and catalytic cracking of PP over 95%Al-HMS catalyst at various temperatures.

	thermal 350°C	thermal 380°C	thermal 410°C	350°C	380°C	410°C
%Conversion	2.4	13.1	76.3	80.3	93.8	94.2
%yield						
%yield 1. gas fraction	2.4	12.1	26.3	25.7	25.3	26.1
2. liquid fraction	-	1.1	50.0	54.7	68.5	68.1
3. residue	97.4	86.9	23.7	19.7	6.2	5.8
- %wax	-	-	-	-	5.2	4.6
- %coke	-	-	-	-	1.0	1.2
%selectivity of liquid fraction						
1. distillate oil	-	-	*25.0*	*37.2*	*53.3*	*49.9*
2. heavy oil	-	-	*75.0*	*62.9*	*46.7*	*50.1*
Total volume of liquid fraction (ml)	-	-	3.1	3.7	4.7	4.7
Liquid fraction density (g/ml)	-	-	0.74	0.73	0.72	0.72

Condition: 10 wt% of catalyst to plastic, N_2 flow of 20 cm^3/min, and reaction time of 30 min. *Deviation within 0.9% for conversion, 0.5% for yield of gas fraction, 0.9% for yield of liquid fraction, and 0.5% for yield of residue.

Figure 4.23 shows the volume of liquid fraction accumulated in the graduated cylinder and the temperature as a function of lapse time. The initial rate of 410°C was much faster than 380°C and 350°C. For at 410°C and 380°C, overall rates of liquid fraction formation were the same. That was due to the temperature dependence on kinetic effect.

The gaseous products from thermal reaction at 350°C-410°C were mainly C_3 (propene), C_5 (n-pentane), C_2 (Ethane), C_4 (iso-butene) and C_5^+ whereas the gaseous products from catalytic reaction were mainly C_3 (propene), C_4 (iso-butane), C_4 (iso-butene), C_5 (iso-pentane) and C_5^+. The data are displayed in Figure. 4.24. The gaseous products

between thermal and catalytic reaction were different because the different mechanism of degradation of polypropylene.

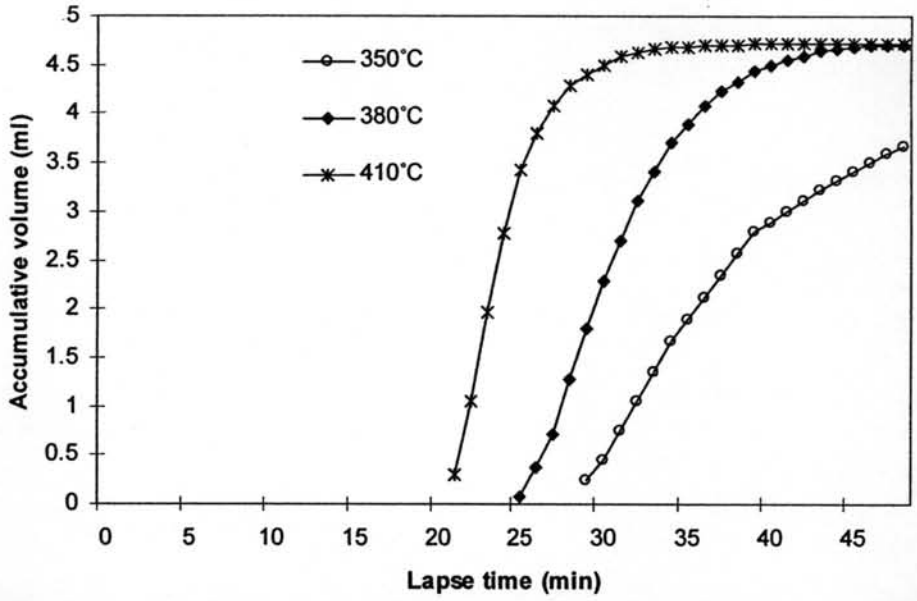

Figure 4.23 Accumulative volume of liquid fractions from catalytic cracking of PP over 95%Al-HMS catalyst at various temperatures.

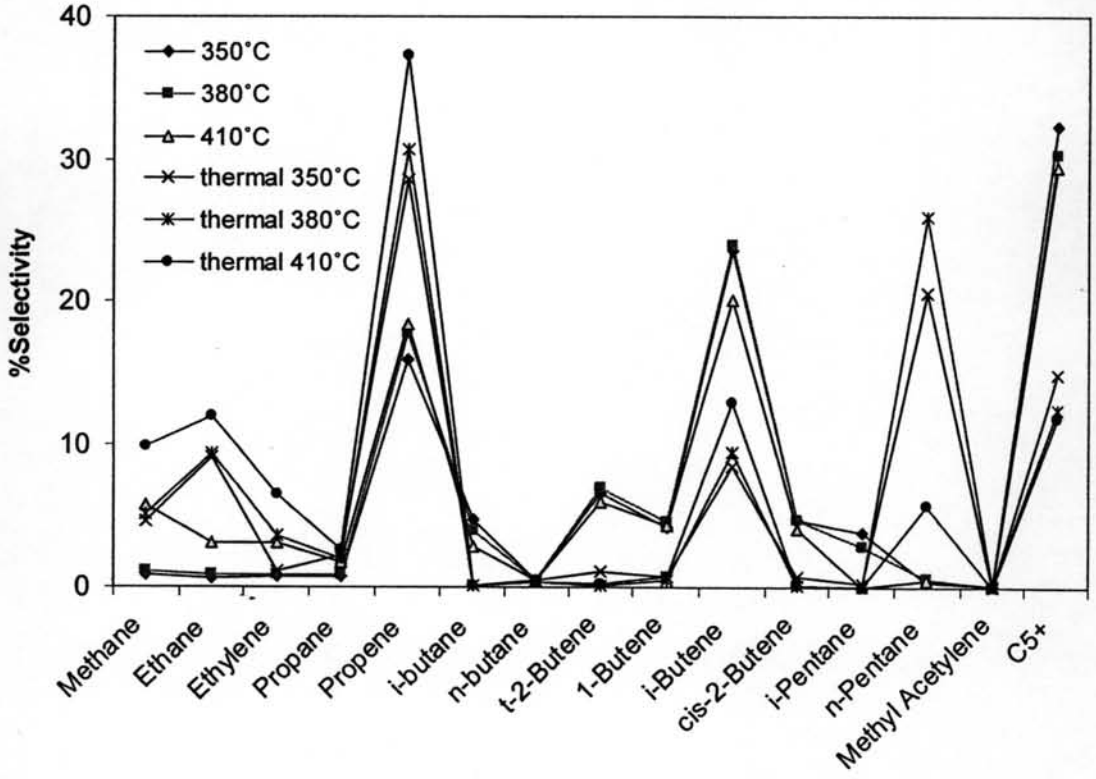

Figure 4.24 Distribution of gas fraction obtained by thermal and catalytic cracking of PP over 95%Al-HMS catalyst at various temperatures.

The liquid products obtained from thermal cracking at 410°C were mainly C_6 and C_9 as shown in Figure 4.26. This result can be explained that the mechanism of thermal cracking performed by free radical mechanism [47]. Some possible reactions are shown as follows:

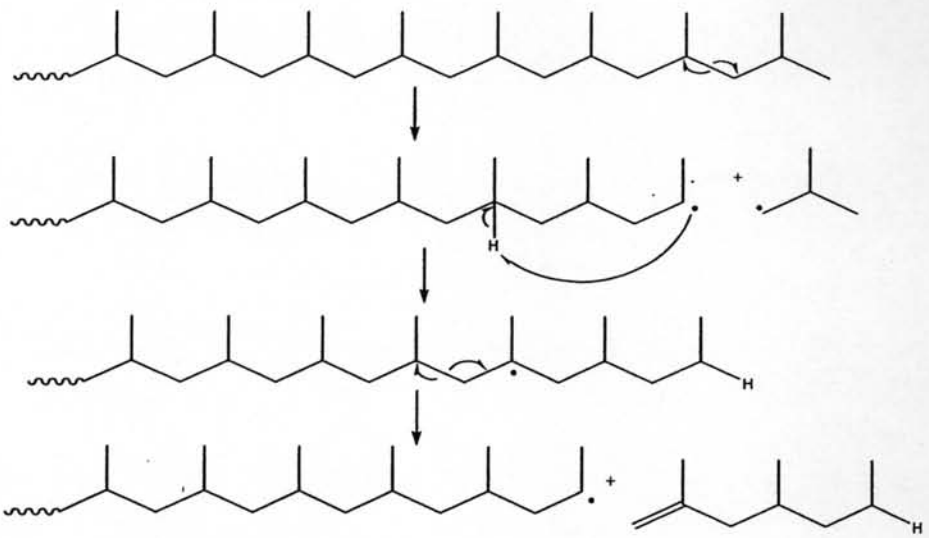

(a)

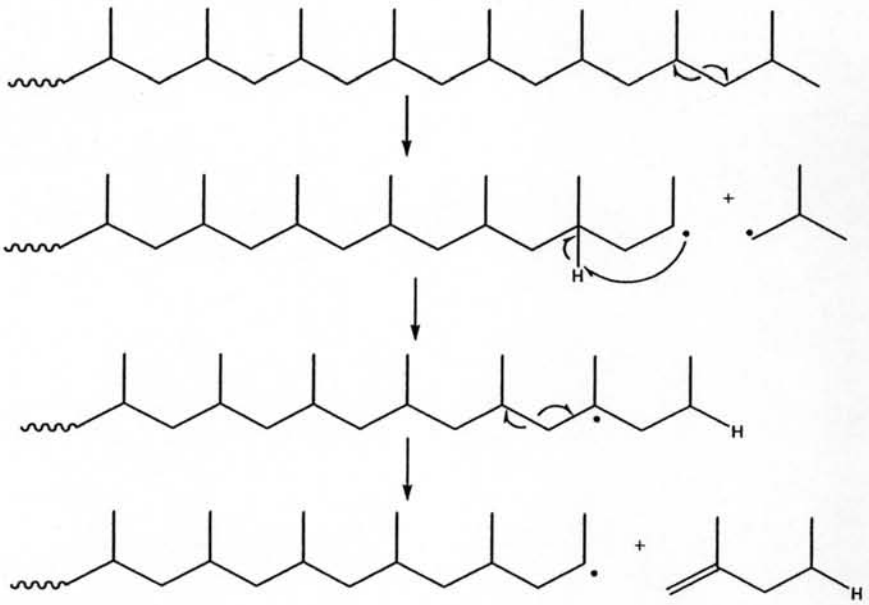

(b)

Figure 4.25 Some possible mechanism of polypropylene cracking (a) C_9 product (b) C_6 product.

Whereas, the major products from catalytic cracking at 350°C-410°C were mainly C_7. This was owing to the selectivity to products of catalysts and the cracking proceeded by carbocation mechanism.

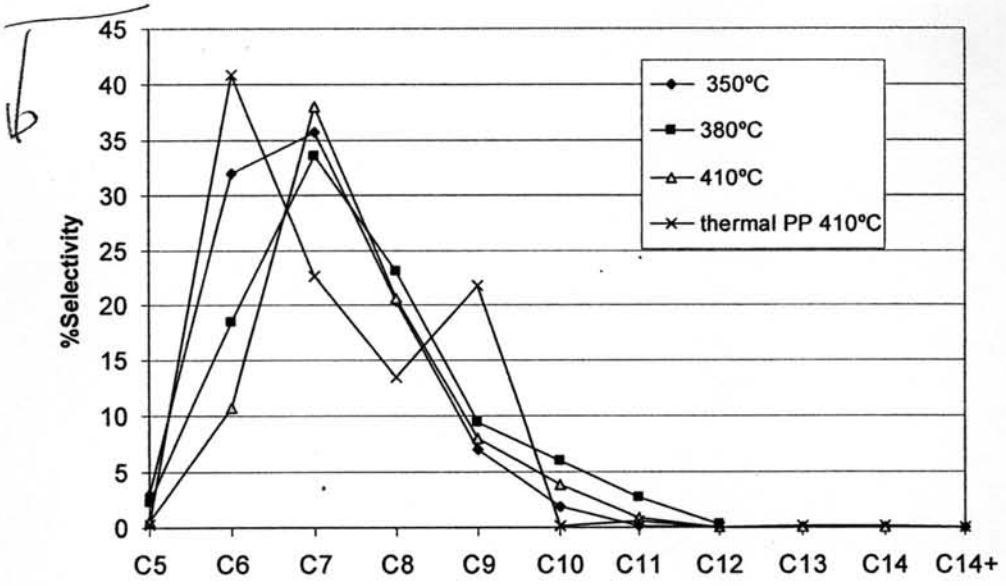

Figure 4.26 Carbon number distribution of distillate oil obtained by thermal and catalytic cracking of PP over 95%Al-HMS at various temperatures.

4.2.3 Catalyst regeneration

The used mixed catalyst with 95%Al-HMS became black after use due to coke deposit on the surface and in the pores. However, it easily turned to white after regeneration by calcination in a muffle furnace at 550°C for 6 h.

The regenerated catalysts were characterized with XRD technique, nitrogen adsorption-desorption technique, NH_3-TPD and the values of %conversion and %yield obtained by the PP cracking using fresh and regenerated 95%Al-HMS catalysts at 380°C are shown in Table 4.9. The BET surface area was slightly decreased while the pore size and acidity was not different. It might be due to the stability of catalyst. Even though the values of %conversion were not different, the regenerated catalyst provided relatively higher yield of gas fraction and lower yield of liquid fraction comparing to the fresh catalyst. In addition, relative more amount of residue, especially in form of wax was remained in the reactor of the regenerated catalyst rather than that of fresh catalyst. This result suggested the structure of regenerated catalyst might be partially collapse as seen in Figure 4.27. The peak intensity of HMS structure decresed after catalyst regenerated.

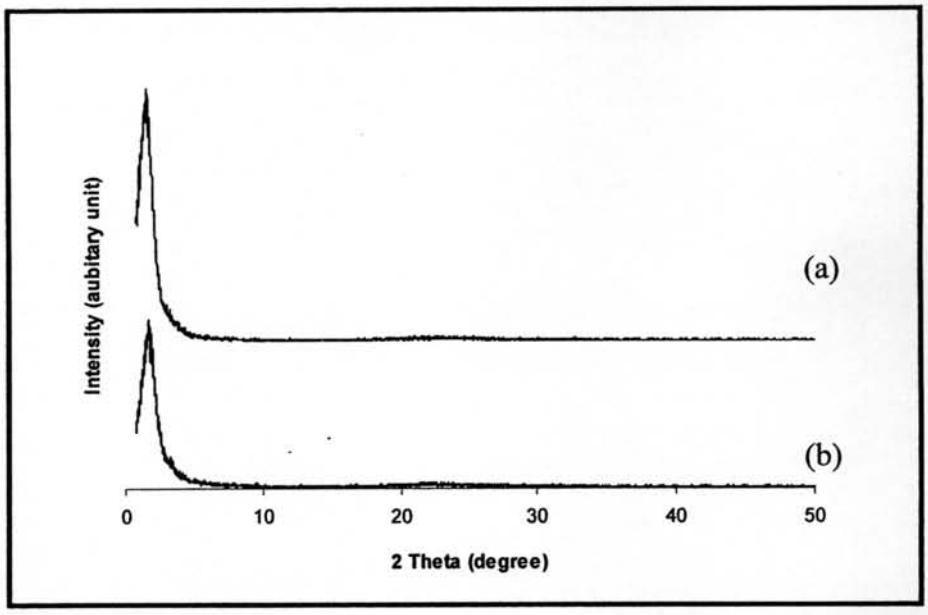

Figure 4.27 XRD patterns of (a) fresh 95%Al-HMS mixed catalyst (b) regenerated 95%Al-HMS mixed catalyst.

Table 4.9 Values of %conversion, %yield, and %selectivity of liquid fraction obtained by catalytic cracking of PP using the fresh and the regenerated 95%Al-HMS mixed catalyst.

	fresh	1st regenerated	2nd regenerated
BET surface area (m^2/g)	782	-	772
Pore size distribution (nm)	4.19	-	4.19
Acidity (mmol/g)	0.46	-	0.40
%Conversion*	93.8	89.6	88.2
%yield* 1. gas fraction	25.3	31.2	31.4
2. liquid fraction	68.5	58.4	56.8
3. residue	6.2	10.5	11.8
- %wax	5.2	9.3	10.2
- %coke	1.0	1.2	1.6
%selectivity of liquid product			
1. distillate oil	*53.3*	*26.1*	*29.2*
2. heavy oil	*46.7*	*73.9*	*70.8*
Total volume of liquid fraction (ml)	4.7	3.8	3.6
Liquid fraction density (g/ml)	0.72	0.73	0.73

Condition: 10 wt% of catalyst to plastic, N_2 flow of 20 cm^3/min, reaction temperature of 380°C, and reaction time of 30 min. *Deviation within 0.9% for conversion, 0.8% for yield of gas fraction, 1.1% for yield of liquid fraction, and 0.8% for yield of residue.

Figure 4.28 shows the accumulative volume of liquid fraction in the graduated cylinder. The rate of liquid formation of fresh catalyst was faster than regenerated.

Figure 4.29 shows distribution of gas fraction obtained by the PP cracking using the fresh and the regenerated 95%Al-HMS catalyst at 380°C. The gas fraction composes of fresh and regenerated catalysts were similar. There was no difference in selectivity in gas fraction between the 1st regenerated and 2nd regenerated but the fresh catalyst gave higher selectivity than both. It was mainly composed of C_3 (propene), C_4 (t-2-butene), C_4 (iso-butene), and C_5^+.

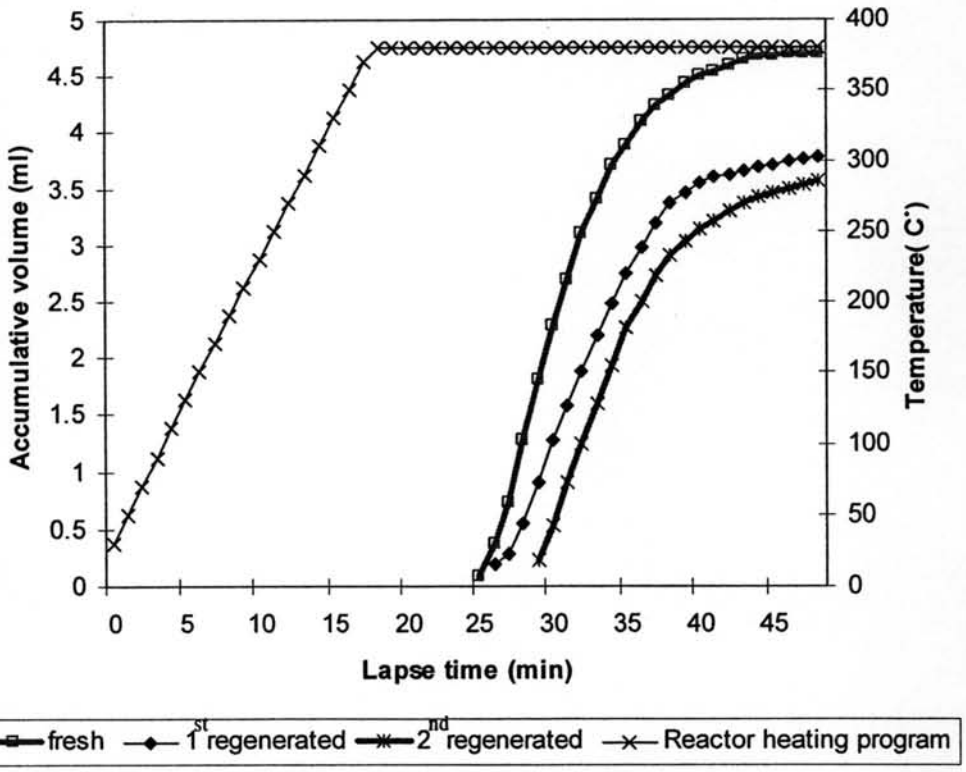

Figure 4.28 Accumulative volume of liquid fraction obtained by catalytic cracking of PP using the fresh and the regenerated 95%Al-HMS mixed catalyst.

Figure 4.30 shows product distribution of the liquid fraction obtained by the PP cracking using the fresh and the regenerated 95%Al-HMS catalyst 380°C. Both fresh and regenerated catalysts provided mainly C_7 in liquid fraction.

In this research, it was concluded that the mixed catalyst with 95%Al-HMS was suitable for the use as cracking catalyst and the used catalyst could be regenerated easily in a furnace. Its cracking activity were slightly decrease.

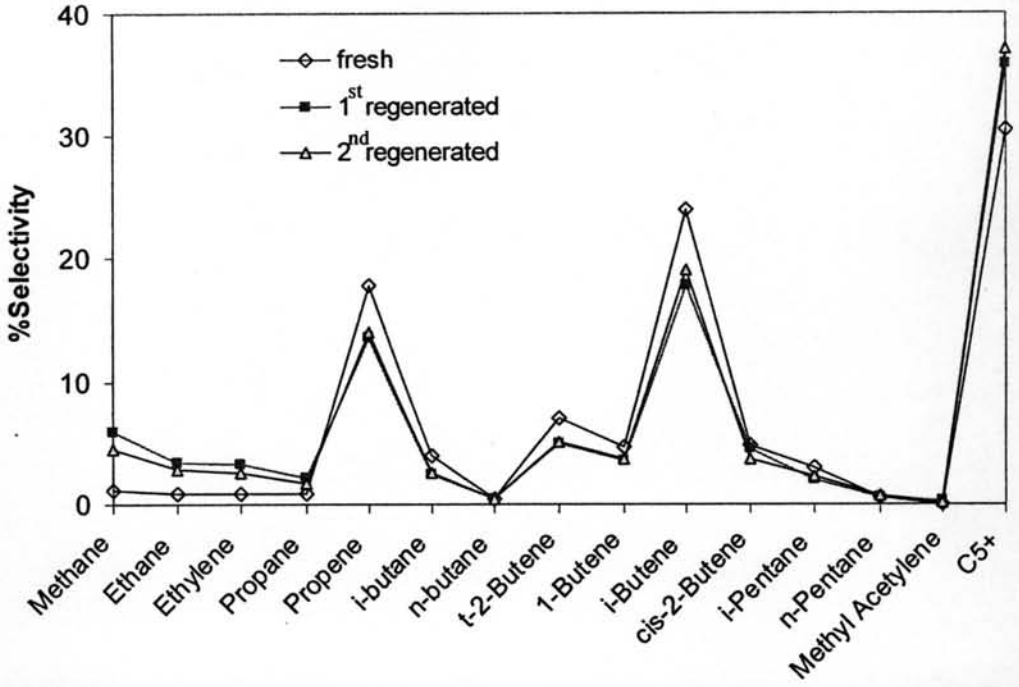

Figure 4.29 Distribution of gas fraction obtained by catalytic cracking of PP over fresh and the regenerated 95%Al-HMS mixed catalyst.

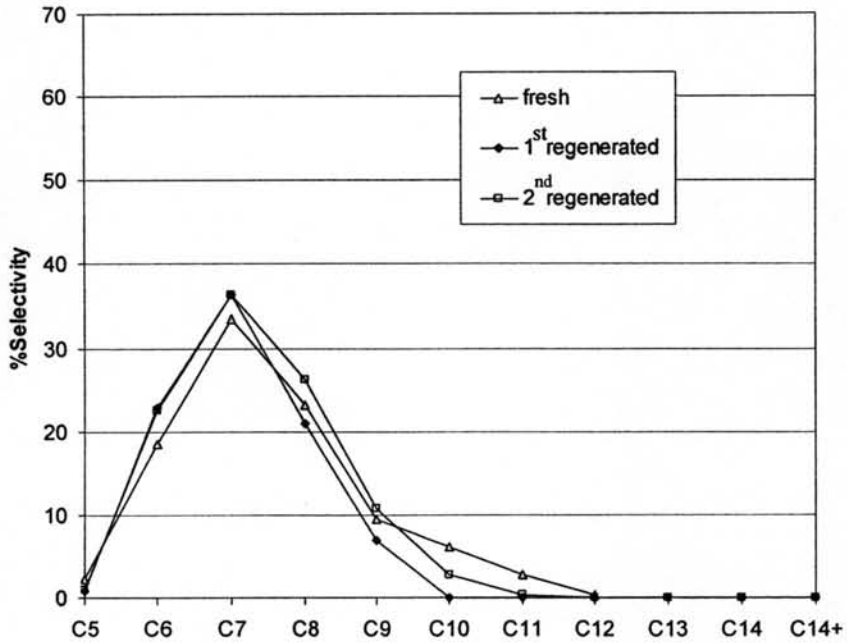

Figure 4.30 Carbon number distributions of liquid fraction obtained by catalytic cracking of PP using the fresh and the regenerated 95%Al-HMS mixed catalyst.

4.3 Activity of catalysts in HDPE cracking

4.3.1 Activity of zeolite beta and Al-HMS mixed catalysts in HDPE cracking

The mixed catalyst were prepared in similar way as in the PP cracking. The physical mixture with various ratios of T1M Al-HMS 40 as follows; 0%Al-HMS, 5%Al-

HMS, 10%Al-HMS, 20%Al-HMS, 40%Al-HMS, 60%Al-HMS, 80%Al-HMS, and 100%Al-HMS. At 0%Al-HMS, it means pure zeolite beta does not mix with T1M Al-HMS 40 and same as 100%Al-HMS which means pure T1MAl-HMS 40 does not mix with zeolite beta.

Table 4.10 shows the catalytic conversion obtained at 380°C in the cracking of HDPE over different ratios of T1M Al-HMS 40 (Al-HMS) comparing with thermal cracking. At 0% Al-HMS (pure zeolite beta) conversion was higher than 100%Al-HMS because the structure of HDPE easily diffused into channel of zeolite and high acidity of zeolite beta was corresponded to the high selectivity of gas fraction. In addition, conversion decreased when the ratio of Al-HMS in mixed catalyst increased. Catalysts in the range of 0-40%Al-HMS gave almost 90% conversion whereas the activities obtained from 60-80%Al-HMS was approximately 80%conversion and activities over 100%Al-HMS were around 68%conversion, which corresponds to the increasing in the residue yield. These results were explained by the structure and properties of microporous material because zeolite beta have a strong acid site and a large number of acidity. Although, the mesopores presented in Al-HMS should favor the diffusion of polyethylene molecules, the order of activities observed suggesting that the major factor influencing the polyethylene cracking was the acidity rather than the pore size of the catalyst. There was no difference in the selectivity to liquid products the acidity played an important role in HDPE cracking. The selectivity to gas products and distillate oil depended on proportion of Al-HMS. With increasing mesoporous content, yield of gas fraction and distillate oil reduced. Thus the acidity of zeolite beta was reduced because of high proportion of Al-HMS.

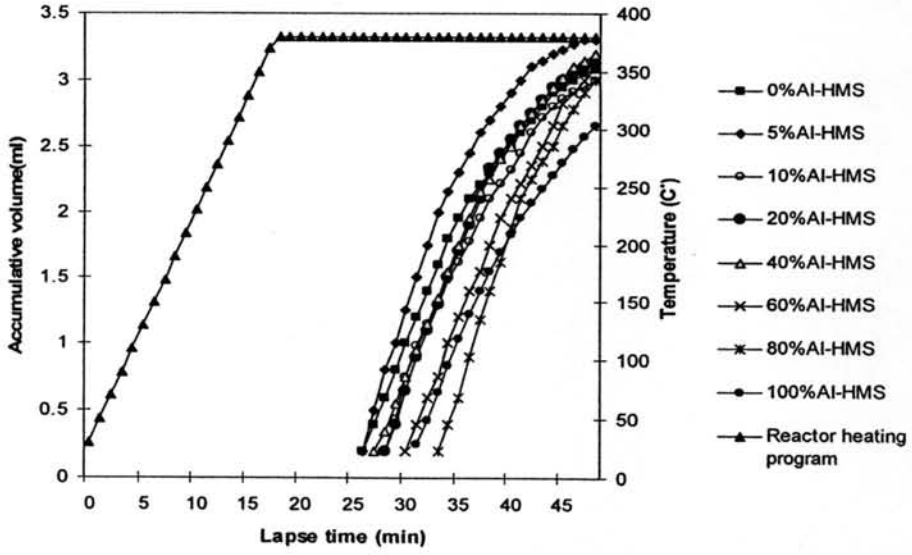

Figure 4.31 Accumulative volume of liquid fractions from catalytic cracking of HDPE over zeolite beta/Al-HMS mixed catalysts with various Al-HMS ratios.

Table 4.10 %Conversion, %yield, and %selectivity of liquid fraction obtained by thermal and catalytic cracking of HDPE over zeolite beta/Al-HMS mixed catalysts with various Al-HMS ratios.

	Thermal	0% Al-HMS	5% Al-HMS	10% Al-HMS	20% Al-HMS	40% Al-HMS	60% Al-HMS	80% Al-HMS	100 Al-%HMS
%Conversion	1.6	88.5	91.5	87.8	86.1	85.9	82.2	77.3	68.4
%yield 1. gasfraction	-	44.7	43.2	41.8	38.9	39.6	36.5	34.1	25.1
2. liquid fraction	-	43.8	48.3	46.0	47.1	46.3	45.7	43.2	43.3
3. residue	98.4	11.5	8.5	12.2	13.9	14.1	17.8	22.7	31.6
%selectivity of liquid product									
1. distillate oil	-	*68.6*	*70.3*	*62.2*	*55.5*	*46.9*	*45.0*	*47.5*	*33.2*
2. heavy oil	-	*31.4*	*29.7*	*37.6*	*44.5*	*53.1*	*55.0*	*52.5*	*66.8*
Total volume of liquid fraction (ml)	-	3.1	3.3	3.0	3.1	3.1	3.1	3.0	3.3
Liquid fraction density (g/ml)	-	0.71	0.72	0.72	0.72	0.72	0.73	0.72	0.74

Condition: 10 wt% of catalyst to plastic, N_2 flow of 20 cm^3/min, reaction temperature of 380°C, and reaction time of 30 min. *Deviation within 0.9% for conversion, 0.5% for yield of gas fraction, 0.9% for yield of liquid fraction, and 0.5% for yield of residue

In this research, it was observed that 5%Al-HMS showed the highest activity. These results could be explained by the mixing of catalysts between microporous and mesoporous materials. HDPE molecules diffused through zeolite pore and broke into the smaller molecules immediately. Whereas the large pore size of Al-HMS allowed large polymer molecules to access the pore and broke the long polymeric chain from ends into small unit or oligomer. Then these oligomer diffused into pore and channel of zeolite and broke into smaller molecules. It was confirmed by cracking rate of mixed catalysts into liquid products, which are displayed in Figure 4.31. The rates of accumulative liquids from HDPE cracking with high proportion of zeolite beta were much faster than the low proportion.

The yields of gaseous products for HDPE cracking are shown in Figure 4.32. Considering only gases at ambient condition which were normally C_1 through C_5, the major component for thermal cracking were C_2 (Ethane), C_3 (propene), C_5 (n-pentane), C_4 (1-butene) and C_5^+. For catalytic cracking major components were C_3 (propene), C_4 (iso-butane), C_4 (iso-butene), C_5 (iso-pentane), C_4 (t-2-butene), and C_5^+. However, the

components C_5^+ from vapor liquids of C_6 (hexane) which had higher boiling point than that of C_5 (n-pentane) was obviously detected in a significant amount.

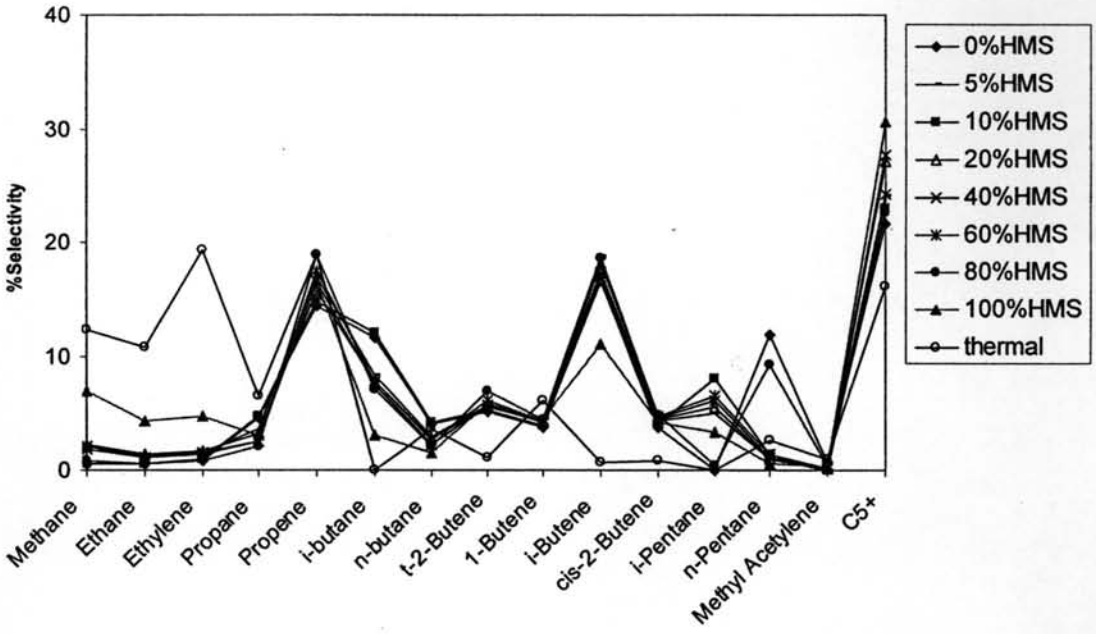

Figure 4.32 Distribution of gas fraction obtained by thermal and catalytic cracking of HDPE over zeolite beta/Al-HMS mixed catalysts with various Al-HMS ratios.

The distribution of liquid products for catalytic cracking of HDPE were found in a broad range of C_6-C_9 as shown in Figure 4.33. It was observed that the main products of catalytic cracking were C_7.

From this experiment, it was concluded that the activity in HDPE cracking over mixed catalyst depended on proportion of microporous material. The effect of the acidity enhanced the activity and distillate oil fraction. However, the selectivity to products varied. If the process required gas and distillate oil product, the higher proportions of zeolite beta were appropriate. Also the process required heavy oil products, the higher proportions Al-HMS were suitable. In this research, 5%Al-HMS gave the highest conversion and high selectivity to liquid product. Therefore, 5%Al-HMS was chosen for further study.

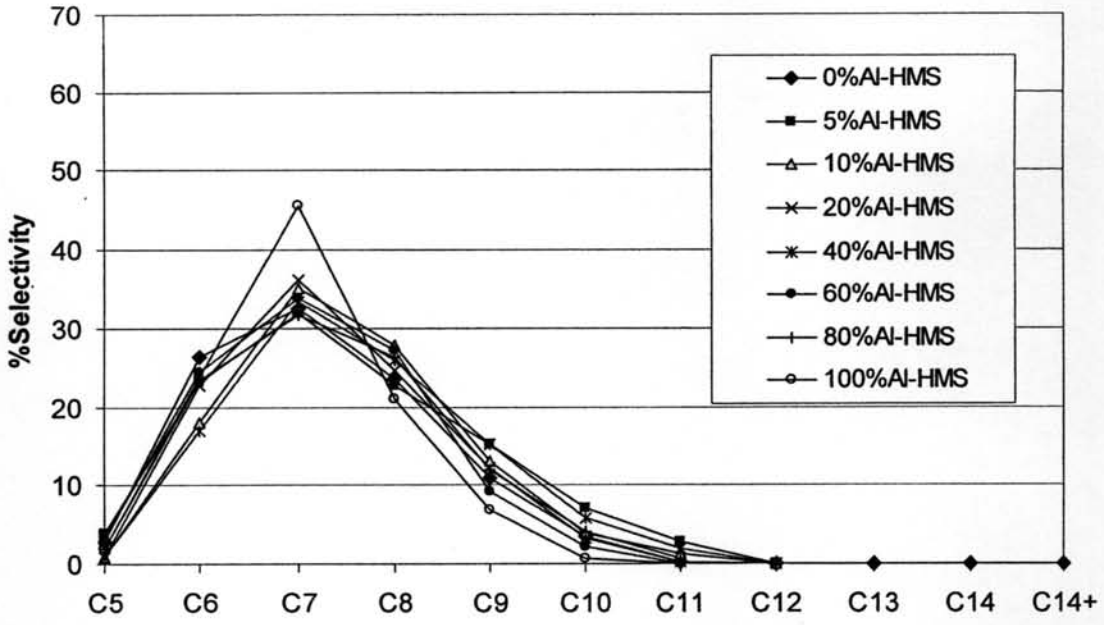

Figure 4.33 Carbon number distribution of distillate oil obtained catalytic cracking of HDPE over zeolite beta/Al-HMS mixed catalysts with various Al-HMS ratios.

4.3.1.1 Effect of plastic to catalyst ratios

To study the effect of plastic to catalyst ratios on the activity mixed zeolite beta/Al-HMS catalysts with 5%Al-HMS was chosen. The variations in plastic to catalyst ratio were studied in the range of 2.5-10% wt. The results are illustrated in Table 4.11. The plastic conversion increased with the catalysts loading in the reaction mixture. An increase in content yielded high conversion. The selectivity to gas fraction and liquid fraction were not much different, while distillate oil increased with increasing the catalyst amount. At 2.5% weight of catalyst, the lowest conversion was observed, which corresponds to residue yields. It was due to the low acidity of catalyst when compared to 5 and 10%weight of catalyst.

Figure 4.34 shows the accumulative volume of liquid products and temperature in reactor as function of lapse time. It was seen that the accumulative liquid for HDPE cracking over 10% weight of catalyst was slightly faster than over 5 and 2.5% weight of catalyst. These suggested that influence of acidity of zeolite beta affected the HDPE cracking.

Table 4.11 %Conversion, %yield, and %selectivity of liquid fraction obtained by catalytic cracking of HDPE over 5%Al-HMS mixed catalyst with various plastic to catalyst ratios.

	2.5%cat	5%cat	10%cat
%Conversion*	89.0	87.8	91.5
%yield*1. gas fraction	38.2	42.6	43.2
2. liquid fraction	50.8	45.2	48.3
3. residue	11.0	12.2	8.5
%selectivity if liquid fraction			
1. distillate oil	47.9	46.5	70.3
2. heavy oil	52.1	53.5	29.7
Total volume of liquid fraction (ml)	3.4	3.3	3.3
Liquid fraction density (g/ml)	0.72	0.72	0.72

Condition: N_2 flow of 20 cm^3/min, reaction temperature of 350°C, and reaction time of 30 min. *Deviation within 0.8% for conversion, 0.8% for yield of gas fraction, 0.6% for yield of liquid fraction, and 0.6% for yield of residue.

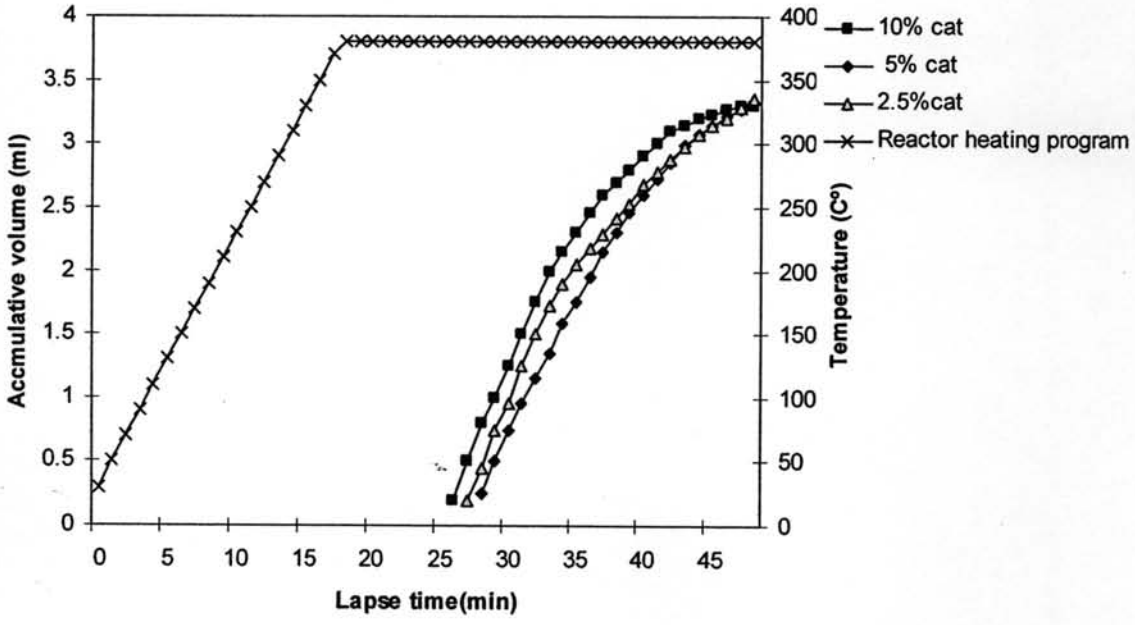

Figure 4.34 Accumulative volume of liquid fractions from catalytic cracking of HDPE over 5%Al-HMS mixed catalyst with various plastic to catalyst ratios.

The yields of gaseous products for HDPE cracking are shown in Figure 4.35. The major components were C_3 (propene), C_4 (iso-butane), C_4 (iso-butene), C_4 (t-2-butene), C_5 (iso-pentane) and high amount of C_5^+.

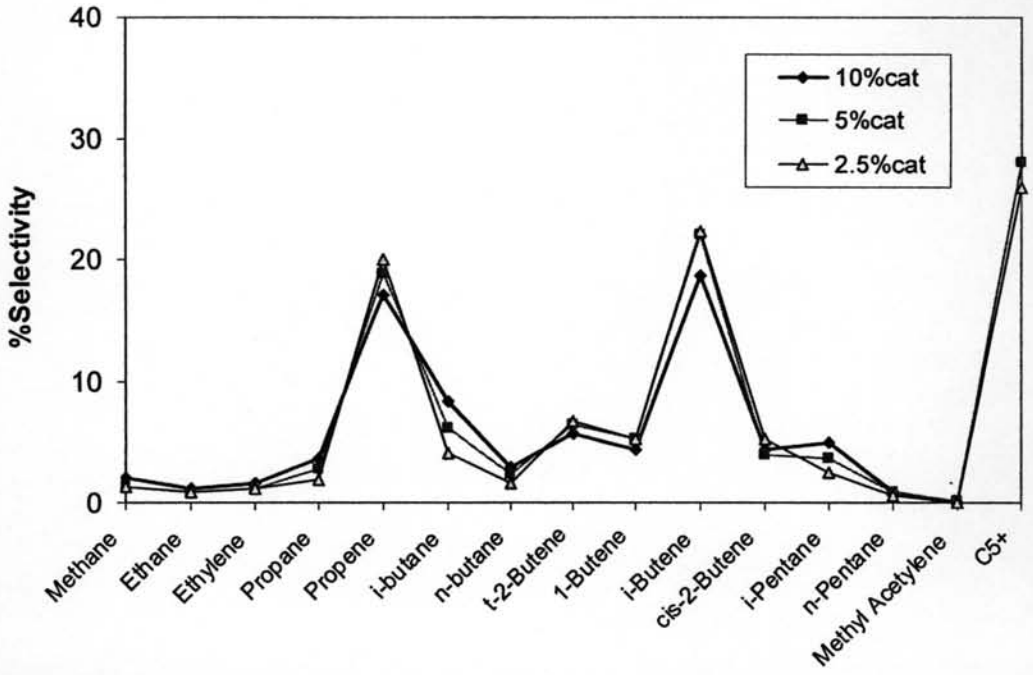

Figure 4.35 Distribution of gas fraction obtained by catalytic cracking of HDPE over 5%Al-HMS mixed catalyst with various plastic to catalyst ratios.

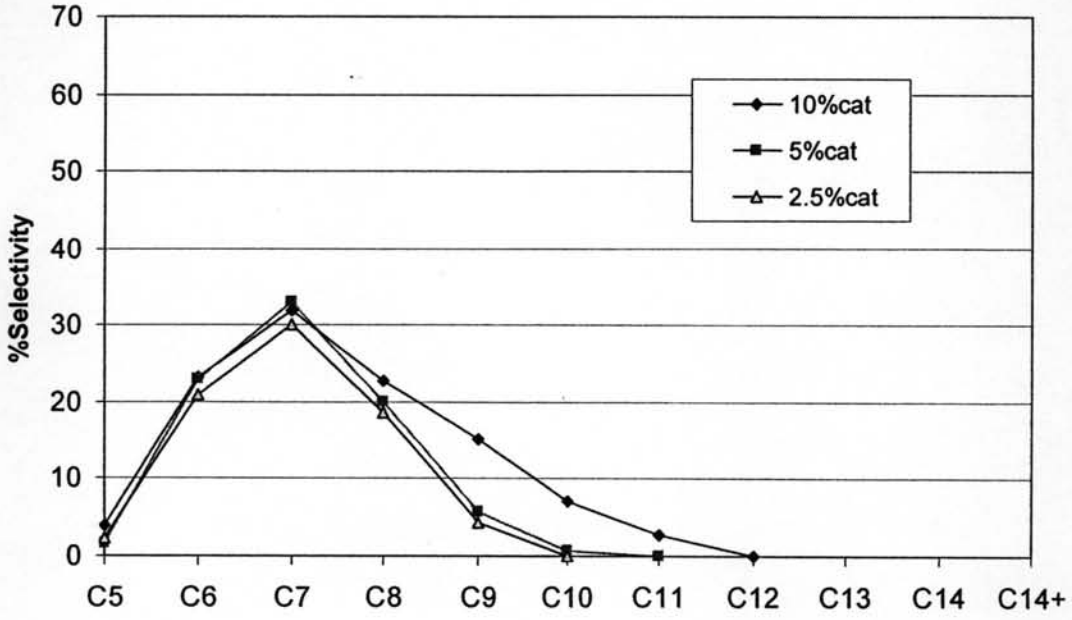

Figure 4.36 Carbon number distribution of distillate oil obtained by catalytic cracking of HDPE over 5%Al-HMS mixed catalyst with various plastic to catalyst ratios.

Figure 4.36 shows the liquid products for catalytic cracking of HDPE were found in broad range of C_5-C_{12}. However, the main products were also C_7, similar to the distribution of commercial gasoline.

According to the results of plastic to catalyst ratio on HDPE cracking, 10%wt of catalyst was selected for further studies due to considerably a high conversion and large amount of liquid fractions obtained.

4.3.1.2 Effect of temperature

The influence of the reaction temperature from 380-410°C were investigated over 5%Al-HMS mixed catalyst with a plastic to catalyst ratio of 10, the result are shown in Table 4.12. For thermal cracking, conversions were increased when temperature increased. It was due to the high temperature enhanced the degradation of polymer. For catalytic cracking, conversion also increased. Comparing the reactions between thermal cracking and catalytic cracking at the same temperature, it was obvious that catalytic cracking showed higher conversion than thermal cracking because the acidity of catalyst increased the degradation of polymer. At 380°C and 410°C, a difference in conversions between catalytic and thermal reaction were 89.9 and 89%, respectively. It was suggested that at 380°C and 410°C, the mixed catalyst exhibited the highest efficiency in HDPE cracking. At 410°C gave higher liquid yield than 380°C.

Figure 4.37 shows the volume of liquid fraction accumulated in the graduated cylinder and the temperature in the reactor as a function of lapsed time. The initial rate of 410°C was much faster than at 380°C. That was due to the temperature dependence of kinetic effect.

In Figure 4.38 the gaseous products of thermal of 380°C and 410°C were similar whereas those of catalytic cracking were mainly composed of C_3 (propene), C_4 (iso-butane), C_4 (iso-butene), C_4 (t-2-butene), C_5 (iso-pentane) and high amount of C_5^+. The liquid products obtained from catalytic cracking at 380°C and 410°C were mainly C_7. The data are displayed in Figure 4.39.

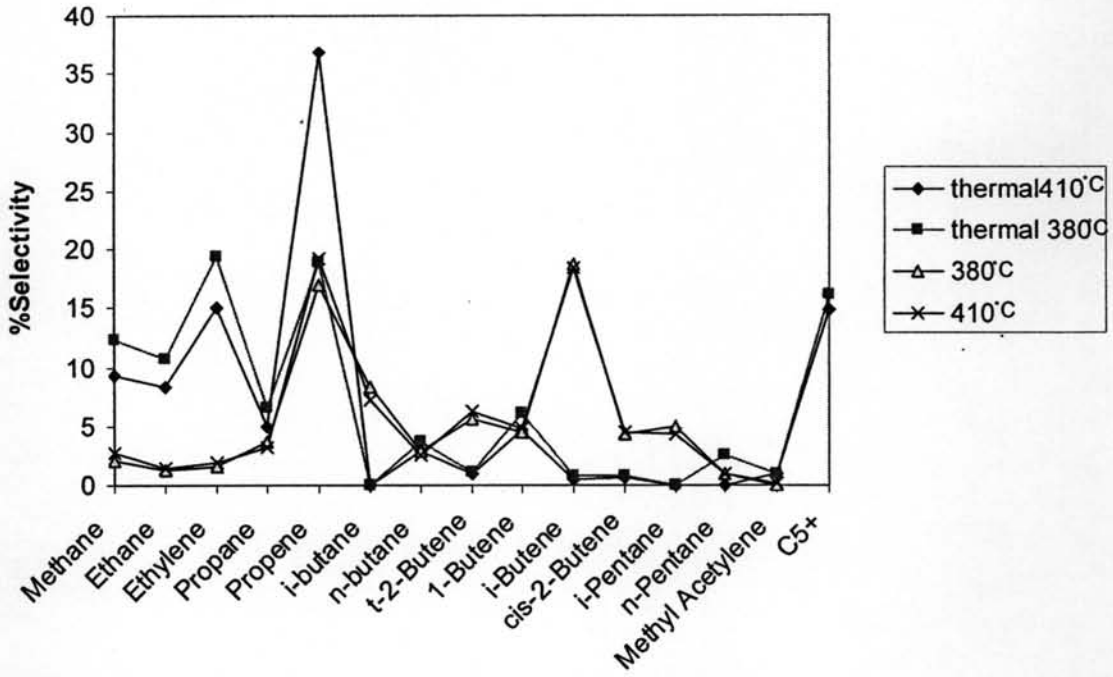

Figure 4.38 Distribution of gas fraction obtained by thermal and catalytic cracking of HDPE over 5%Al-HMS mixed catalyst with various temperatures.

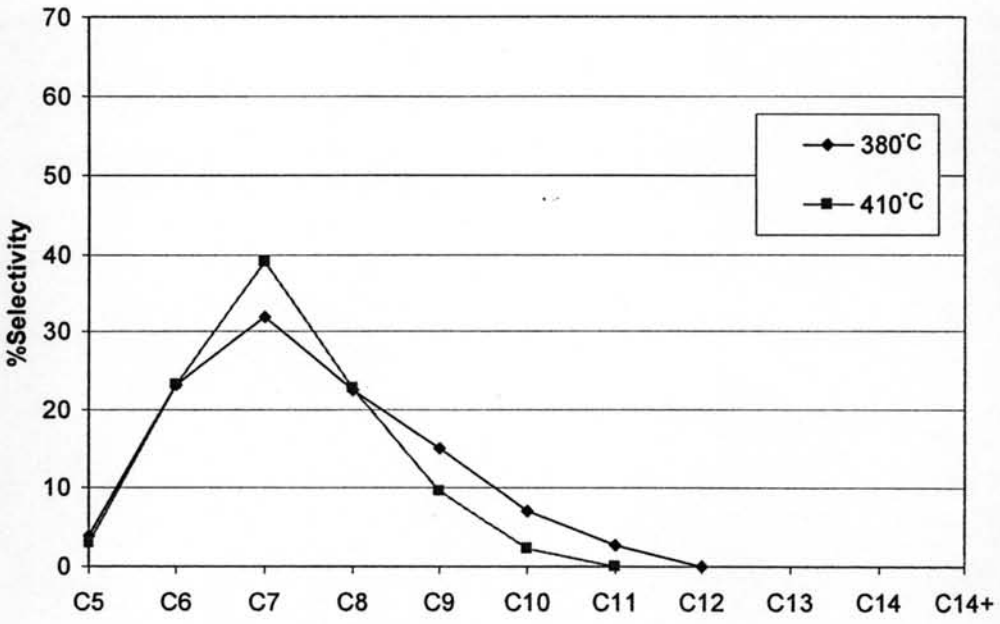

Figure 4.39 Carbon number distribution of distillate oil obtained by catalytic cracking of HDPE over 5%Al-HMS mixed catalyst with various temperatures.

4.3.2 Catalyst regeneration

The used mixed catalyst with 5%Al-HMS became black after use due to coke deposit on the surface and in the pores. However, it easily turned to white after regeneration by calcination in a muffle furnace at 550°C for 6 h.

The regenerated catalysts were characterized with XRD technique, nitrogen adsorption-desorption technique, NH_3-TPD and the values of %conversion and %yield obtained by the HDPE cracking using fresh and regenerated 5%Al-HMS catalysts at 410°C are shown in Table 4.13. The intensity peak of fresh and regenerate catalyst were not different as seen in Figure 4.40. The BET specific surface area and acidity were decreased. The pore size was not decreased. The values of %conversion were different, the significant differences are the yield ratio of distillate oil and heavy oil. The regenerated catalyst provided lower yield of distillate oil comparing to the fresh catalyst. In addition, relatively more amount of residue, especially in form of wax was remained in the reactor of the regenerated catalyst rather than that of fresh catalyst. This result may be implied that the external surface area of regenerated catalyst were blocked by coke or the alumination of atoms from the tetrahedral framework may be possible.

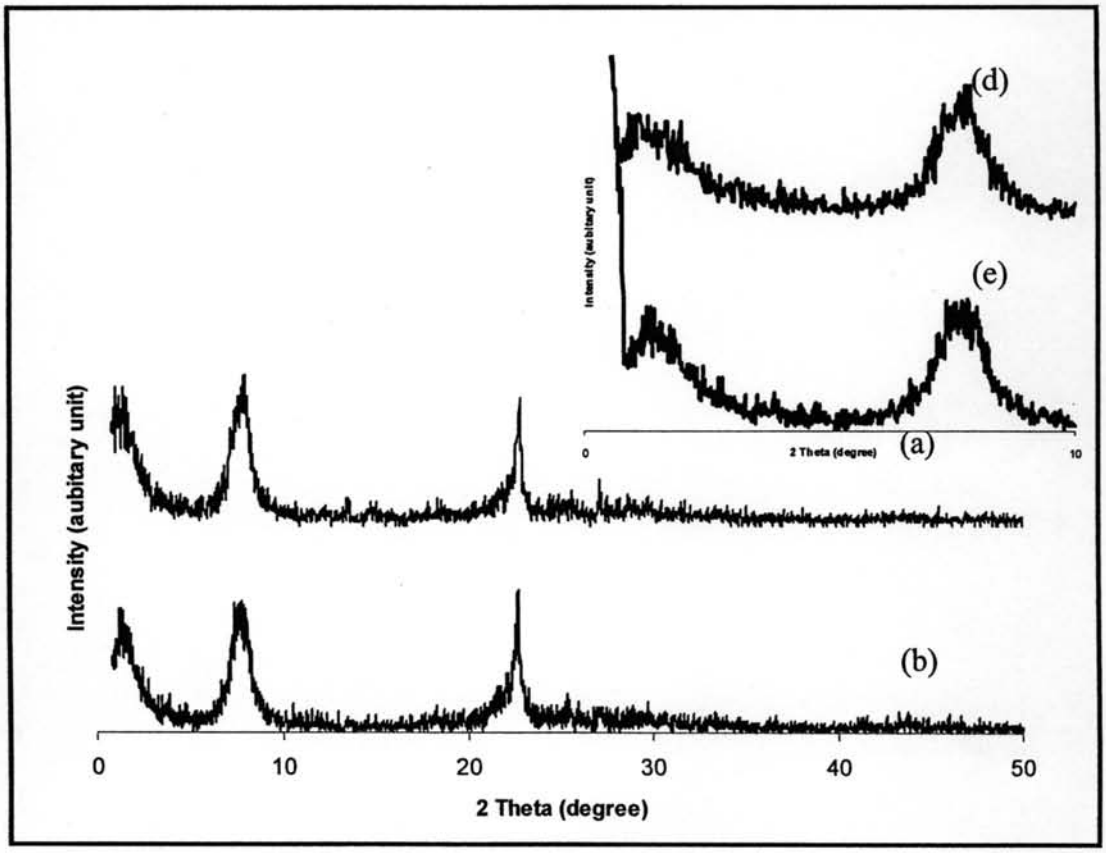

Figure 4.40 XRD patterns of (a)-(d) fresh 5%Al-HMS mixed catalyst (b)-(e) regenerated 5%Al-HMS mixed catalyst.

Table 4.12 %Conversion, %yield, and %selectivity of liquid fraction obtained by thermal and catalytic cracking of HDPE over 5%Al-HMS mixed catalyst with various temperatures.

	thermal 380°C	thermal 410°C	380°C	410°C
%Conversion*	1.6	6.8	91.5	95.8
%yield* 1. gas fraction	1.6	6.8	43.2	39.8
2. liquid fraction			48.3	56.0
3. residue	98.4	93.2	8.5	4.2
%selectivity of liquid fraction				
1. distillate oil	-	-	70.3	67.6
2. heavy oil	-	-	29.7	32.4
Total volume of liquid fraction (ml)	-	-	3.3	4.0
Liquid fraction density (g/ml)	-	-	0.72	0.72

Condition: 10 wt% of catalyst to plastic, N_2 flow of 20 cm^3/min, and reaction time of 30 min. *Deviation within 0.9% for conversion, 0.5% for yield of gas fraction, 0.9% for yield of liquid fraction, and 0.9% for yield of residue.

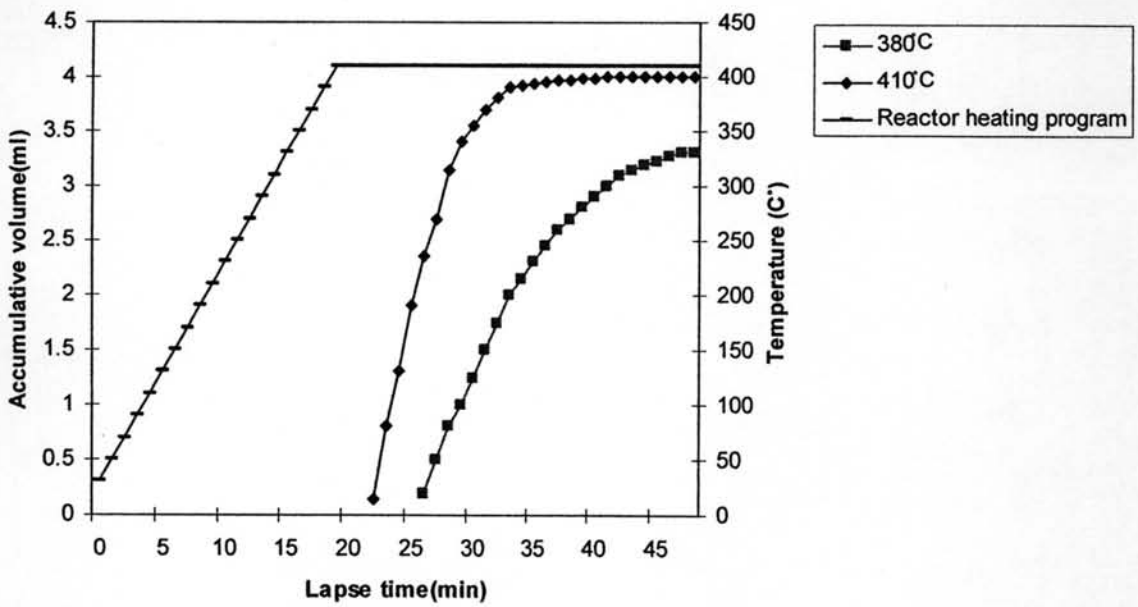

Figure 4.37 Accumulative volume of liquid fractions from catalytic cracking of HDPE over 5%Al-HMS mixed catalyst with various temperatures.

Table 4.13 %Conversion, %yield, and %selectivity of liquid fraction obtained by catalytic cracking of HDPE using the fresh and the regenerated 5%Al-HMS mixed catalyst.

	Fresh	1st regenerated	2 nd regenerated
BET surface area (m^2/g)	768	-	745
Pore size (nm)	0.6	-	0.6
Acidity (mmol/g)	0.70	-	0.51
%Conversion*	95.8	89.6	89.2
%yield* 1. gas fraction	39.8	36.9	34.1
2. liquid fraction	56.0	57.8	55.1
3. residue	4.2	5.3	10.8
- % wax	3.2	4.0	9.2
- %coke	1.0	1.3	1.6
%selectivity of liquid fraction			
1. distillate oil	67.6	47.8	46.9
2. heavy oil	32.4	52.2	53.1
Total volume of liquid fraction (ml)	4.0	4.2	3.9
Liquid fraction density (g/ml)	0.72	0.72	0.73

Condition: 10 wt% catalyst of plastic, N_2 flow of 20 cm^3/min, 410 °C, and reaction time of 30 min. *Deviation within 0.8% for conversion, 0.6% for yield of gas fraction, 0.9% for yield of liquid fraction, and 0.7% for yield of residue.

Figure 4.42 shows distribution of gas fraction obtained by the HDPE cracking using the fresh and the regenerated 5%Al-HMS catalyst at 410°C. The gas fraction components of fresh and regenerated catalysts were similar. There was no difference in selectivity in gas fraction between fresh and regenerated catalyst. They were mainly composed of C_3 (propene), C_4 (iso-butane), C_4 (iso-butene), C_4 (t-2-butene), C_5 (iso-pentane) and high amount of C_5^+.

Figure 4.43 shows product distribution of the liquid fraction obtained by the HDPE cracking using the fresh and the regenerated 5%Al-HMS catalyst at 410°C. Both fresh and regenerated catalysts provided mainly C_5 to C_{11} range in liquid fraction whereas the major products was C_7.

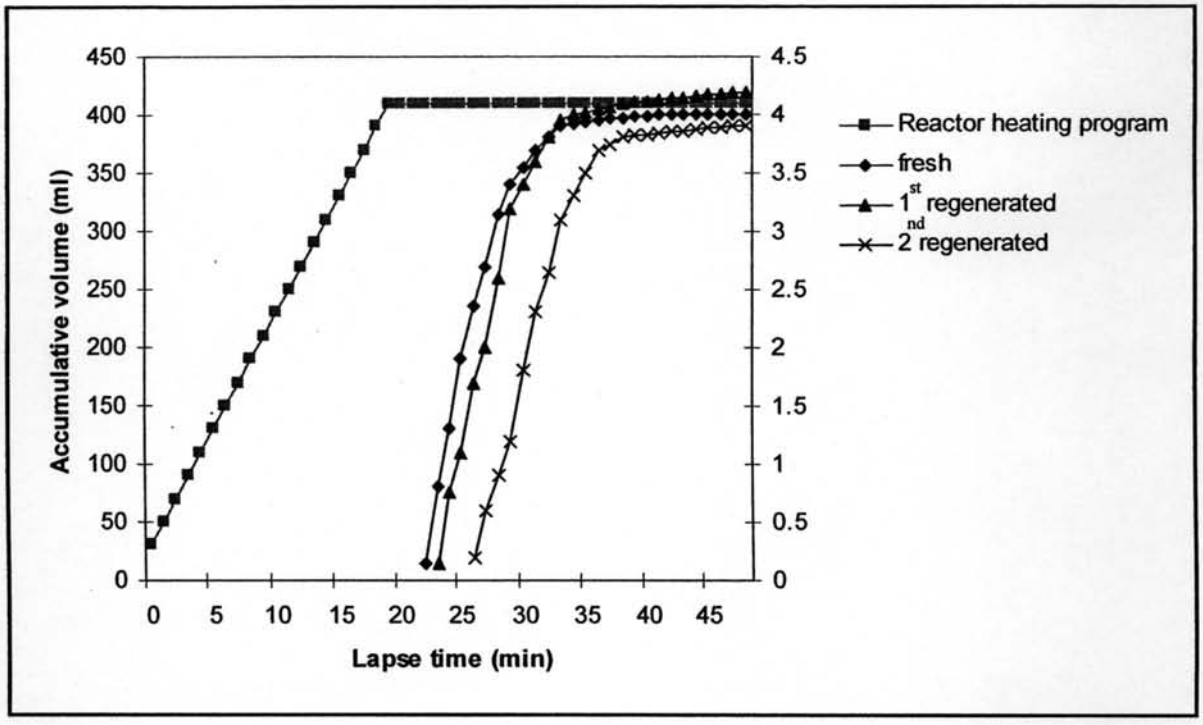

Figure 4.41 Accumulative volume of liquid fraction obtained by catalytic cracking of HDPE using the fresh and the regenerated 5%Al-HMS catalyst.

Figure 4.41 shows the accumulative volume of liquid fraction in the graduated cylinder. The rate of liquid formation of fresh catalyst is faster than regenerated.

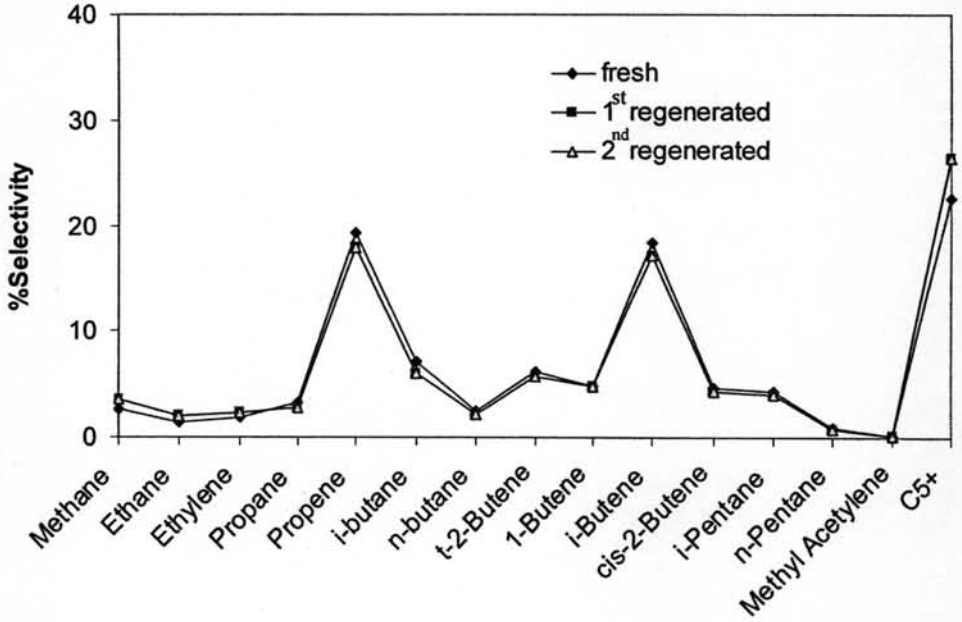

Figure 4.42 Distribution of gas fraction obtained by catalytic cracking of HDPE over fresh and the regenerated 5%Al-HMS catalyst.

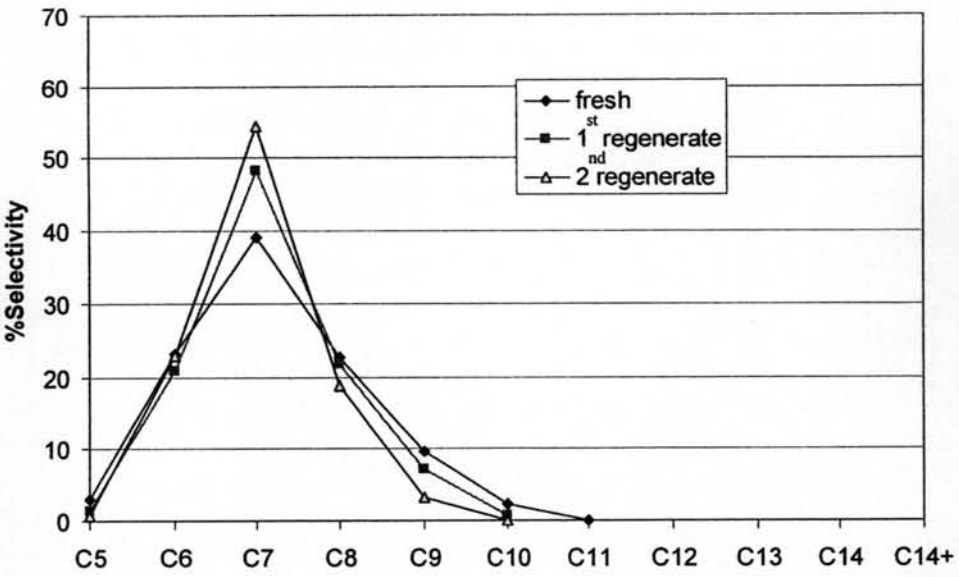

Figure 4.43 Carbon number distributions of liquid fraction obtained by catalytic cracking of HDPE using the fresh and the regenerated 5%Al-HMScatalyst.

In this research, it was concluded that the 5%Al-HMS used catalyst could be regenerated easily in a furnace. Its cracking activity was acceptable due to a high conversion in HDPE cracking over 80%. The distribution of gas and liquid products were similar to the fresh catalyst.